Theses and Dissertations                        1. Thesis and Dissertation Collection, all items

2010-12

# MAXIMIZING AVAILABLE DIVERSITY IN A MIMO FADING CHANNEL

## NG, Wei Gee

Monterey, California. Naval Postgraduate School

http://hdl.handle.net/10945/70936

# NAVAL POSTGRADUATE SCHOOL

## MONTEREY, CALIFORNIA

# THESIS

**MAXIMIZING AVAILABLE DIVERSITY IN A MIMO FADING CHANNEL**

by

NG Wei Gee

December 2010

| | |
|---|---|
| Thesis Co-Advisors: | Tri. T. Ha |
| | Weilian Su |

**Approved for public release; distribution is unlimited**

THIS PAGE INTENTIONALLY LEFT BLANK

| **1. AGENCY USE ONLY** *(Leave blank)* | **2. REPORT DATE** December 2010 | **3. REPORT TYPE AND DATES COVERED** Master's Thesis |
|---|---|---|

| **4. TITLE AND SUBTITLE** Maximizing Available Diversity in a MIMO Fading Channel | | **5. FUNDING NUMBERS** |
|---|---|---|
| **6. AUTHOR(S)** NG Wei Gee | | |

| **7. PERFORMING ORGANIZATION NAME(S) AND ADDRESS(ES)** Naval Postgraduate School Monterey, CA 93943-5000 | **8. PERFORMING ORGANIZATION REPORT NUMBER** |
|---|---|

| **9. SPONSORING /MONITORING AGENCY NAME(S) AND ADDRESS(ES)** N/A | **10. SPONSORING/MONITORING AGENCY REPORT NUMBER** |
|---|---|

**11. SUPPLEMENTARY NOTES** The views expressed in this thesis are those of the author and do not reflect the official policy or position of the Department of Defense or the U.S. Government.  IRB Protocol number: N/A.

| **12a. DISTRIBUTION / AVAILABILITY STATEMENT** Approved for public release; distribution is unlimited | **12b. DISTRIBUTION CODE** |
|---|---|

**13. ABSTRACT (maximum 200 words)**
The effects of Rayleigh fading on a wireless communications link and the diversity techniques that are available to combat fading are explored in this thesis. The thesis consists of two main portions; an exploration on the use of spatial diversity and an exploration on the use of space-frequency diversity.

In harnessing spatial diversity, the use of space-time coding is proposed to combat fading. Several codes of diversity two and four are explored, including Quasi-Orthogonal (QO) codes that are able to achieve a unity rate. The concept of constellation rotation for QO codes to maximize the available diversity is studied. QO codes are shown by simulation to be able to achieve full diversity, despite the fact that the codes are non-orthogonal.

The use of space-time-frequency (STF) code to harness both space and frequency diversity is also explored. Simulations were performed for a variety of channel correlations to simulate varying degrees of frequency-selectivity. Results show that STF codes are very effective when the correlations in frequency response are less than 0.5. STF codes also have a power advantage over space-time codes with comparable diversity and bandwidth efficiency.

| **14. SUBJECT TERMS** MIMO, Rayleigh Fading Channels, Diversity, Space-Time Code, Quasi-Orthogonal Space-Time Code, Constellation Rotation, Space-Time-Frequency Code | **15. NUMBER OF PAGES** 99 |
|---|---|
| | **16. PRICE CODE** |

| **17. SECURITY CLASSIFICATION OF REPORT** Unclassified | **18. SECURITY CLASSIFICATION OF THIS PAGE** Unclassified | **19. SECURITY CLASSIFICATION OF ABSTRACT** Unclassified | **20. LIMITATION OF ABSTRACT** UU |
|---|---|---|---|

THIS PAGE INTENTIONALLY LEFT BLANK

# MAXIMIZING AVAILABLE DIVERSITY IN A MIMO FADING CHANNEL

NG Wei Gee
Military Expert 5, Republic of Singapore Air Force
B.Eng (EEE), Nanyang Technological University, 2001

Submitted in partial fulfillment of the
requirements for the degree of

**MASTER OF SCIENCE IN ELECTRICAL ENGINEERING**

from the

**NAVAL POSTGRADUATE SCHOOL
December 2010**

Author:          NG Wei Gee

Approved by:     Tri T. Ha
                 Thesis Co-Advisor

                 Weilian Su
                 Thesis Co-Advisor

                 R. Clark Robertson
                 Chairman, Department of Electrical and Computer Engineering

THIS PAGE INTENTIONALLY LEFT BLANK

# ABSTRACT

The effects of Rayleigh fading on a wireless communications link and the diversity techniques that are available to combat fading are explored in this thesis. The thesis consists of two main portions, an exploration on the use of spatial diversity and an exploration on the use of space-frequency diversity.

In harnessing spatial diversity, the use of space-time coding is proposed to combat fading. Several codes of diversity two and four are explored, including Quasi-Orthogonal (QO) codes that are able to achieve a unity rate. The concept of constellation rotation for QO codes to maximize the available diversity is studied. QO codes are shown by simulation to be able to achieve full diversity, despite the fact that the codes are non-orthogonal.

The use of space-time-frequency (STF) code to harness both space and frequency diversity is also explored. Simulations were performed for a variety of channel correlations to simulate varying degrees of frequency-selectivity. Results show that STF codes are very effective when the correlations in frequency response are less than 0.5. STF codes also have a power advantage over space-time codes with comparable diversity and bandwidth efficiency.

THIS PAGE INTENTIONALLY LEFT BLANK

# TABLE OF CONTENTS

# LIST OF FIGURES

THIS PAGE INTENTIONALLY LEFT BLANK

# LIST OF TABLES

THIS PAGE INTENTIONALLY LEFT BLANK

# LIST OF ACRONYMS AND ABBREVIATIONS

| | | | |
|---|---|---|---|
| ASK | Amplitude Shift Keying | OFDM | Orthogonal Frequency Division Multiplexing |
| AWGN | Additive White Gaussian Noise | OFDMA | Orthogonal Frequency Division Multiple Access |
| BER | Bit Error Rate | PEP | Pairwise Error Probability |
| BPSK | Binary Phase Shift Keying | QAM | Quadrature Amplitude Modulation |
| C2 | Command and Control | | |
| C4I | Command, Control, Communications, Computer and Intelligence | QO | Quasi-Orthogonal |
| | | QPSK | Quadrature Phase Shift Keying |
| CR | Constellation Rotation | SIMO | Single-Output Multiple-Input |
| ICI | Inter-Carrier Interference | SNR | Signal-to-Noise Ratio |
| ISI | Inter-Symbol Interference | STBC | Space-Time Block Codes |
| MIMO | Multiple-Input Multi-Output | STF | Space-Time-Frequency |
| MISO | Multiple-Input Single-Output | STFC | Space-Time-Frequency Codes |
| ML | Maximum Likelihood | | |
| MRC | Maximal-Ratio Combining | | |
| NCW | Network Centric Warfare | | |

THIS PAGE INTENTIONALLY LEFT BLANK

# EXECUTIVE SUMMARY

Wireless communications present a distinct set of challenges as the signal has to propagate through an unguided medium. This results in severe attenuation and uncontrollable wave propagation effects such as scattering, diffraction, and refraction. The receiving antenna usually receives multiple copies of the original signal that are distorted as they travel through the air via *multipaths*. The multipath effect can produce either constructive or destructive interferences that result in changes to the amplitude, frequency, and phase of the original signal. Such distortions on the signal, known as *fade,* can have a significant detrimental effect on the reliability of the communications link.

In order to combat such effects, *diversity* techniques can be employed whereby the transmitter sends multiple copies of the signal via the time, frequency or spatial domain with the hope that the receiver will be able to successfully decode at least one copy of the signal.

The various fading conditions and methods to harness the available diversity depending on the channel conditions are explored in this thesis. The research primarily focuses on exploiting spatial diversity with space-time block codes (STBC) as well as space-frequency diversity with space-time-frequency (STF) codes.

For harnessing the spatial diversity, two classes of codes are investigated. Orthogonal STBC have a simple decoding structure and can achieve full spatial diversity but are unable to achieve full code rate beyond a diversity order of two. Quasi-orthogonal (QO) STBC can achieve full code rates for any diversity order but have a complex decoding structure and are unable to achieve full spatial diversity in their native form.

Some researchers have proposed the use of constellation rotation (CR) as an effective means to restore the full diversity that is potentially available in QO-STBC. A mathematical analysis to determine the optimum angle of rotation to achieve full diversity through a quantity known as the diversity product is presented in this thesis. Simulations were then run for varying angles of rotation to validate the mathematical analysis. During the course of this study, the author made an interesting observation that

while the diversity product is a sufficient statistic for full diversity, it was not a necessary one. Several angles of rotation with poor diversity product and expected to have a poor bit error rate (BER) performance predicted by the mathematical analysis turned out to perform on par with angles that achieved full diversity.

The research then compares the performance of orthogonal STBC to the best performing QO-STBC. The two classes of codes perform on par when compared for the same bandwidth efficiency with lower order modulations, but QO-STBC out-performs the orthogonal STBC with higher order modulations.

The process of achieving diversity in both the space and frequency domains was then investigated. The author analyzed the performance of the STF codes based on the frequency-selectivity of the channel and performed simulations with varying degrees of correlation between the channel taps. Results showed that when the correlation between the taps was less than 0.5, the BER performance closely matched that of completely independent channel taps. The author also performed further studies using a fading channel model to better understand the relationship between channel tap correlations and coherence bandwidth, which is typically defined as the bandwidth for 50% correlation. The study shows that completely uncorrelated channel taps require a very large frequency separation between the subcarriers and would be difficult to achieve. With the results from the study that the 50% correlation BER curves closely match those of the uncorrelated curves, it becomes clear why the coherence bandwidth is defined for 50% correlation (and not any smaller bandwidth) is sufficient for good diversity performance.

Finally, the performance of the STBC and the STF codes were compared. The STF codes were shown to have a 3 dB advantage over the STBC given the same bandwidth efficiency and diversity order. This is because STBC require twice the number of antennas as the STF codes and therefore each signal from every antenna in the STBC transmitter only has half the power compared to the STF code. The STF codes, on the other hand, "spread" its diversity across both the spatial and frequency domains. Therefore, the results show that harnessing simultaneous diversity in multiple domains can be beneficial for the communications link. However, that requires that the channel condition be suitable (i.e., frequency-selective) for frequency diversity to be available. In

addition, the modulator and demodulator would have to be more complex, as the STF codes require the use orthogonal frequency-division multiple access (OFDMA) subcarriers in order to send the signal across different frequencies.

THIS PAGE INTENTIONALLY LEFT BLANK

# ACKNOWLEDGMENTS

I would like to express my heartfelt appreciation to my thesis advisor, Prof Tri Ha, for his unwavering patience and guidance during my research and analysis for this thesis. Thank you for being open to ideas and giving me to freedom to implement and choose the direction with which the thesis was heading, which during the course of the thesis, changed several times. Thank you for bringing me back to the ground when my ideas started running wild and ensuring that the thesis could be completed on time.

Most importantly, I would like to thank my wife, Selene, for her relentless support and patience in taking care of me during one of the most stressful times of my life. In between struggling with the household chores and taking care of the kid, she has never forgotten to ensure that my needs were well taken care of. She has also taken upon herself all of the administrative chores so as to relieve me of the maximum available time to concentrate on my studies. Thank you, dear.

Lastly, I would like to thank my son, Kai Kiat, for being the inspiration and joy in my life.

THIS PAGE INTENTIONALLY LEFT BLANK

# I.     INTRODUCTION

## A.     BACKGROUND

Communication systems have an extremely important role in the conduct of any military operation. The heart of network centric warfare (NCW) lies in the C4I (Command, Control, Communications, Computer and Intelligence) system. Therefore, reliable and robust communication links are the key to the success of a NCW concept.

Communication systems can either be wired or wireless. Wired systems are employed where extensive infrastructure can be built up beforehand and are required over a long time. These are typically used in command and control (C2) systems with strategic importance. Some examples of wired communication systems include C2 command centers, operating bases, and key communications infrastructure such as network and communication backbones. Wireless systems, on the other hand, are used where mobility is required or when time and accessibility to an area of operations are limited and do not allow for the setup of a wired communications architecture. Therefore, tactical communications links such as those found in operating units, sensor, and weapon systems typically use wireless communications link.

Wireless communications present a distinct set of challenges that affect their link reliability. This is predominantly due to the fact that as the wireless signal travels through the air, it suffers severe attenuation (due to the unguided nature of the medium), interference (from competing sources), various atmospheric effects (such as diffraction, refraction and scattering), as well as other geometric effects (movement of transmitters and receivers or the environment, interference due to multipath). All of these effects result in a random fluctuation of the received signal's strength. This fluctuation can result in periods when the signal strength falls below the detectable threshold, which lead to a complete loss of communication. This fluctuation is called *fade* ([1] – [3]), and periods of complete outage are called *deep fade*. A wireless communications link that is experiencing fading can perform poorly, even when the bit error rate (BER) performance

1

predicted by a simple additive white Gaussian noise (AWGN) channel is very good. Fading is a unique phenomenon experienced by a wireless channel that is typically not found in wired communications.

Fading can be overcome with *diversity*. Diversity is a technique that sends multiple copies of a message from the transmitter to the receiver in order to improve the reliability of the transmission. This is based on the premise that simultaneous outages will not occur on the multiple copies. The message can be replicated in the time, frequency, or spatial domains.

Since Alamouti's landmark paper ([4]) on transmit diveristy, there has been considerable research into harnessing transmit diversity from all domains, including the spatial domain ([5]–[12]), space-frequency domain ([13]–[16]) and space-time-frequency domain ([17], [18]). In each of these papers, the researchers address the various challenges of harnessing the available diversity given the available channel conditions.

## B.    OBJECTIVES OF THE STUDY

In this thesis, we will study the diversity gains that are possible under different channel fading conditions. First, the various modes of fading due to the delay and Doppler spread of a signal are reviewed. The various diversity techniques that are available to combat the different types of fading channels are then explored. The efficacies of these techniques are validated via simulations in Matlab. The notion of maximizing the available diversity given a multiple-input multiple-output (MIMO) system based on the current fading conditions is also investigated.

## C.    SCOPE AND ORGANIZATION OF THE THESIS

This thesis is limited to the study of quasi-static channels and the maximization of the available diversity in the space and frequency domains only. The thesis is divided into two main portions. Spatial diversity is explored in the first part, while space-frequency diversity is explored in the second.

A brief review of the fading channels and various diversity techniques for different fading conditions is given in Chapter II. The theory of spatial diversity as well

as the simulation results is covered in Chapters III and IV. The theory of space-frequency diversity as well the simulation results is covered in Chapters V and VI. Lastly, a conclusion and recommendations for future work is provided in Chapter VII.

THIS PAGE INTENTIONALLY LEFT BLANK

## II.     FADING CHANNELS AND DIVERSITY TECHNIQUES

### A.     FADING CHANNELS

When a wireless signal propagates through space, it experiences wave propagation effects such as reflection, refraction, and scattering due to the environment. The receiving antenna thus receives multiple copies of the signal with varying delays due to the different paths that the signal propagate through. This effect is known as *multipath propagation*. An example of how a signal sent from the transmitter experiences multipath propagation through the environment before it reaches the receiver is shown in Figure 1.
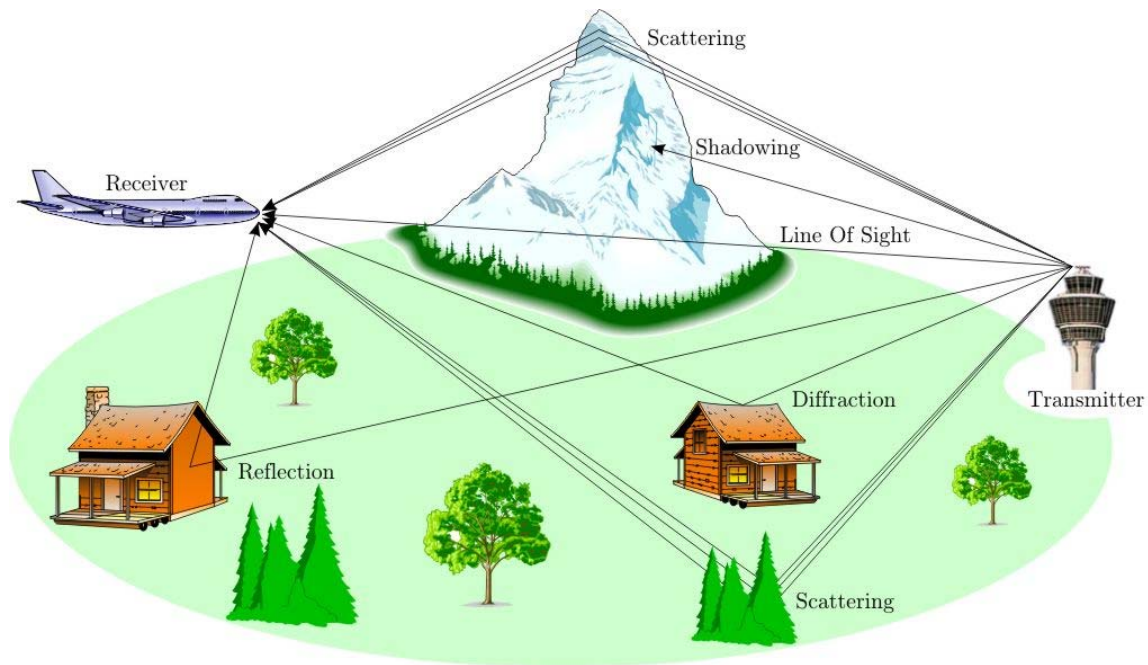


Figure 1.     Example of multipath propagation (From [19]).

When a receiver receives the combined effects of all the multipath waves, it experiences what is known as *fading*. The fading effect at the receiver results in changes to the magnitude, phase, and frequency of the signal at the point of sampling. These changes result from the interference of the multipath waves, which can be either constructive (in phase) or destructive (out of phase), as well as the relative motion between the transmitter and receiver or motion of the environment. The various fading

characteristics are briefly described in the following sections. Several different textbooks, for example, [1] – [3], provide a more thorough treatment on fading.

### 1.     Multipath Delay Spread and Coherence Bandwidth

A wireless signal that experiences multipath effects reaches the receiver via different path lengths and arrives at different times with varying signal strengths. A profile of the delay and strength can be measured and characterized into a *power-delay profile*. The *delay spread* can be calculated as the standard deviation of the power-delay profile, which is denoted as $\sigma_\tau$. Hence, delay spread is the amount of spreading that a signal experiences in a specific environment. An example of a power-delay profile, using the six-ray Typical Urban (TU) model from COST 207 ([20]), is shown in Figure 2.
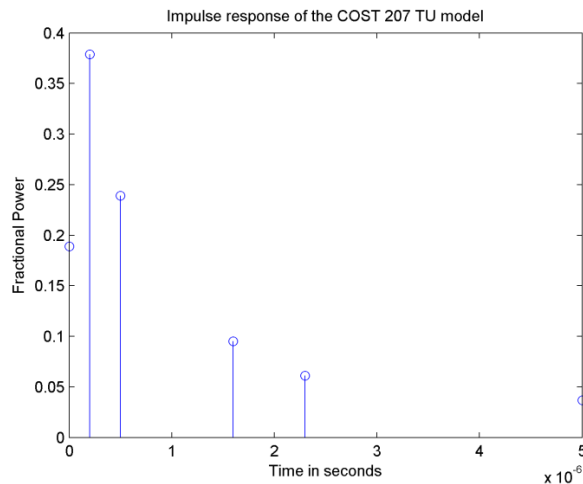


Figure 2.     Sample of a power-delay profile.

The delay spread of a signal can cause problems when the residual energy from a previous symbol is added to the current symbol being detected. This results in inter-symbol interference (ISI). One parameter employed to establish the effects of delay spread is the *coherence bandwidth* of the channel. The relationship between the delay spread and the coherence bandwidth is empirical and depends on the channel. For the purpose of this thesis, the coherence bandwidth in [21] is as follows:

$$B_c = \frac{1}{5\sigma_\tau} \tag{2.1}$$

where $B_c$ is the coherence bandwidth and $\sigma_\tau$ is the delay spread. Coherence bandwidth can be viewed as the bandwidth which the fading attenuation is constant and phase shifts are linear. Any signal bandwidth which is smaller than the coherence bandwidth is said to experience a *frequency-flat fading*. If the signal bandwidth is larger than the coherence bandwidth, then the signal is said to experience a *frequency-selective fading*, which can result in non-linear distortion of the signal and ISI which can be difficult to correct.

### 2. Doppler Shift and Coherence Time

The relative motions between the transmitter and receiver or the environment introduces Doppler shifts on each of the multipath waves. These shifts result in changes to the frequency of the transmitted signal. The amount of Doppler shift is given as $f = f_c v / c$, where $f_c$ is the center frequency of the signal, $v$ is the relative velocity, and $c$ is the speed of light (typically given as $3 \times 10^8$ m/s). At the receiver, the received signal has a range of frequency shifts, which is termed the *Doppler spread*. The Doppler spread is the difference between the maximum and minimum frequency changes amongst all of the multipath waves and can be given as in [1]:

$$f_D = \max_{i,j} \left| f_i - f_j \right| \tag{2.2}$$

where $f_D$ is the Doppler frequency and $f_i$ and $f_j$ denotes the maximum and minimum frequency shifts amongst all of the multipaths. For simplicity, the maximum Doppler shift can also be defined as $f_{D_{max}} = f_c v_{max} / c$, where $v_{max}$ is the maximum radial velocity between the transmitter and receiver. This results in a Doppler spread of $2f_{D_{max}}$. The center frequency of a transmitted signal may then be spread across the range of $f_c \pm f_{D_{max}}$. If the Doppler spread is too high, it may result in *inter-carrier interference* (ICI) where energy from one carrier (frequency) is carried across to another carrier (frequency).

From the definition of Doppler spread, the coherence time $T_c$ can be defined as ([1])

$$T_c = \frac{1}{4f_D}. \tag{2.3}$$

7

Coherence time is the approximate timeframe in which the channel exhibits correlated fading. From (2.3), it is clear that if there is no Doppler shift in the channel, the coherence time is infinite. This implies that the channel is time-invariant. However, time-invariant channels do not exist in reality due to the movement in the environment and/or the transmitter and receiver. Therefore, any symbol time that is smaller than the coherence time experiences *slow fading*, while any symbol time that is larger than the coherence time experiences *fast fading*.

### 3. Summary of Fading Characteristics

The fading characteristics of a channel is summarized in Table 1, while a graphical view of how the channel gain varies with respect to the time and frequency domain under various fading conditions is shown in Figure 3.

Table 1.    Summary of fading characteristics.

| | Signal bandwidth $< B_c$ (Flat fading) | Signal bandwidth $> B_c$ (Frequency-selective fading) |
|---|---|---|
| **Symbol time $< T_c$ (Slow fading)** | Negligible ISI<br>Negligible ICI | Significant ISI<br>Negligible ICI |
| **Symbol time $> T_c$ (Fast fading)** | Negligible ISI<br>Significant ICI | Significant ISI<br>Significant ICI |

In Figure 4, the effect of a flat Rayleigh fading channel on the bit error rate (BER) performance on a wireless transmission versus a standard additive white Gaussian noise (AWGN) channel is shown. As can be observed from Figure 4, the BER for the Rayleigh channel deviates from the AWGN significantly as the $E_b / N_0$ increases. This illustrates that fading has a significant effect on the reliability of a wireless communications channel and needs to be addressed accordingly to ensure reliable communications between sender and recipient.
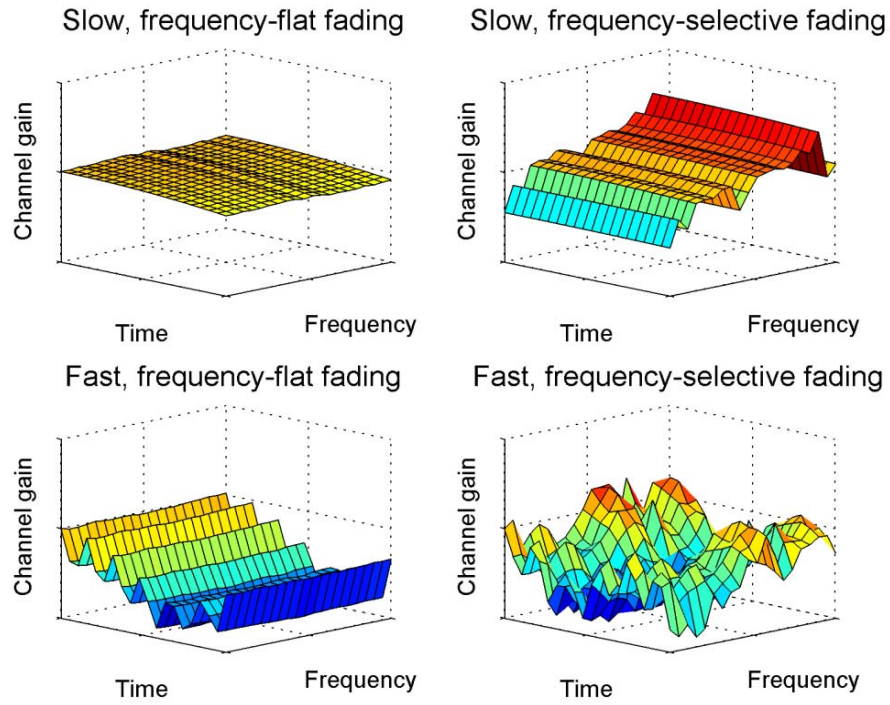
Figure 3.    Graphical view of channel gain under various channel fading conditions.
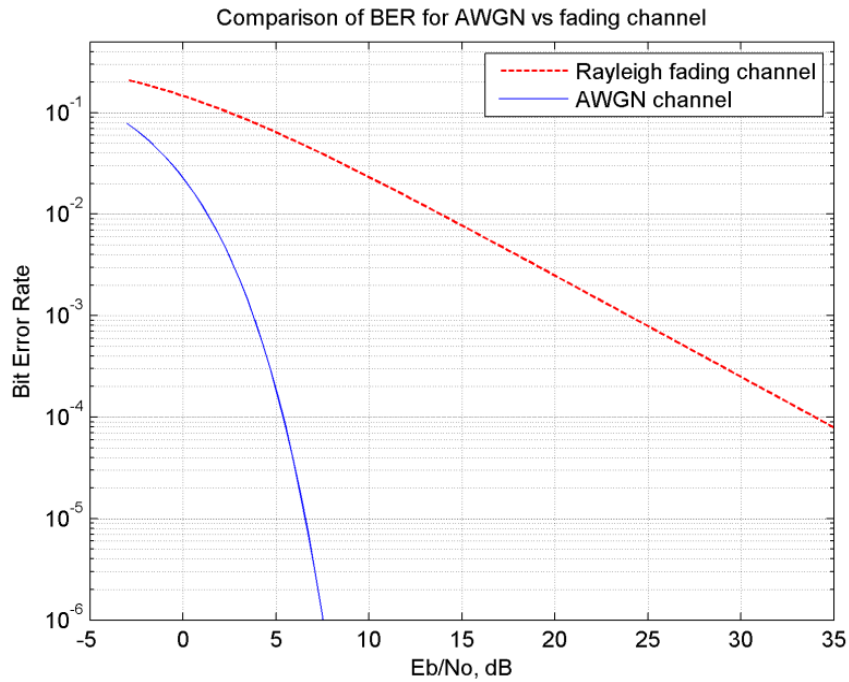


Figure 4.    BER of Rayleigh fading channel versus AWGN channel.

## B.     DIVERSITY TECHNIQUES

Any form of wireless communications will experience fading to some extent due to the geometry of the environment. During deep fades, it is possible for the signal-to-noise ratio (SNR) of a channel to fall below that of an operational threshold and, thus, experience an outage of a communication link. In order to combat fading, diversity techniques have been devised to improve the reliability of a communications link and lower the possibility of outages. The basic concept of diversity is to send multiple copies of the same symbol via multiple uncorrelated channels with the hope that at least one copy of the symbol will arrive at the receiver with sufficient SNR to be decoded correctly. Diversity techniques are widely discussed in various literatures, e.g., [1] − [3], [21]. It is not hard to deduce that the probability of having simultaneous outages on all uncorrelated channels is very small. For example, given an outage probability of 0.1 on any channel, a modest diversity of two can decrease the outage probability from 0.1 to 0.01, i.e., the probability of outages on both channels simultaneously is 0.01[1]. Therefore, one can see that diversity is a powerful technique that significantly improves the reliability of a communications link.

Diversity can be implemented in three different domains: time, frequency, and space. This implies that one can choose to replicate a symbol across any combination of these three domains to increase the diversity beyond one (i.e., no replication). The different types of diversity are further explained in the following sections.

### 1.     Time Diversity

Time diversity is achieved by replicating symbols in different time slots. In order for the channels to be uncorrelated, the minimum separation between the replicated symbols has to be greater than the coherence time of the channel. This ensures that the replicated symbol does not experience the same fading conditions as the original symbol

---

[1] This is assuming that each of the channel outage probability remains the same after diversity is implemented. In reality, this may not necessarily be true. For example, if two antennas are used for spatial diversity, the power of the transmitted signal on each channel will be half that of a single antenna. This may result in a lowered SNR for each channel, which may raise the outage probability. However, in the case of high SNR, diversity has been shown to significantly increase the reliability of a wireless link ([14], [13], [9]).

and, thus, reduces the probability of simultaneous outages on both symbols. One way of implementing time diversity is through the use of an interleaver, which is usually combined with some form of error correction coding. However, in time-sensitive applications such as telephony, the delays introduced by time diversity may be intolerable. Therefore, time diversity may be suited to a fast fading channel where the channel conditions change rapidly and coherence time is small. One drawback of time diversity is the reduction in bandwidth due to the need to replicate symbols in the time domain, which could have been used to transmit a different symbol.

### 2.    Frequency Diversity

Frequency diversity uses different frequencies to transmit multiple copies of the same symbol simultaneously. For frequency diversity to be effective, the fading conditions experienced by different frequencies must be uncorrelated. Therefore, frequency diversity is only suited for a frequency-selective channel. Several methods of implementing frequency diversity are currently employed. They include spread spectrum, frequency-hopping, and multicarrier modulation schemes. Frequency diversity also results in a loss of bandwidth efficiency similar to time diversity.

### 3.    Spatial Diversity

Spatial diversity is the replication or detection of symbols using multiple antennas on the transmitter and/or the receiver. Depending on where the multiple antennas are implemented, we can have *transmit diversity* (also known as multiple-input, single-output, or MISO, as seen from the receiver end), *receive diversity* (also known as single-input, multiple-output, or SIMO), or both (also known as MIMO). Spatial diversity has gained a lot of popularity in recent years because it preserves bandwidth efficiency and does not require the allocation of additional time or frequency for diversity. However, spatial diversity requires a more complicated transmitter or receiver due to the need to incorporate additional hardware such as antennas and modulators. In order for spatial diversity to be effective, the paths taken by the symbols through the multiple antennas have to experience uncorrelated fading. This can be implemented either by spacing the

antennas sufficiently far apart (usually in the order of a few wavelengths) to achieve *angular diversity* or using different polarization on the different antenna to achieve *polarization diversity*.

## C. DIVERSITY COMBINING METHODS

The combination of time, frequency, and spatial diversity can create higher orders of diversity. When the receiver receives multiple copies of the symbol, it must decide how to combine the copies into a form that can be deciphered into data. The receiver can use various methods of combining the signals such as *selection combining*, *switched combining*, *equal-gain combining* and *maximal-ratio combining* (MRC). Each method has its own advantages and disadvantages. The details of various combining techniques are beyond the scope of this thesis, and interested readers may peruse literature such as [1], [3] and [22] for details.

# III. SPATIAL DIVERSITY

Since Alamouti's landmark paper on a class of space-time block codes with simple decoding complexity ([4]), there has been considerable research into designing codes with higher orders of diversity as well as exploiting diversity in the spatial, time, and frequency domains simultaneously (for example, [5] – [18]). The performance of a few space-time block codes that harness spatial diversity with varying degrees of diversity is explored in this chapter.

## A.   SPACE-TIME BLOCK CODES

Given a quasi-static, frequency-flat fading MIMO system with $n$ transmit antenna and $m$ receive antenna, a space-time block code can exploit the spatial diversity with a diversity order equivalent to $nm$ provided that each spatial path from each pair of transmit-receive antennas experiences independent fading characteristics from one another. A MISO system can be seen as a special case of MIMO, when $m = 1$, i.e., there is only one receiving antenna on the receiver end. This is usually the case for portable communications devices, which communicate with a base station, when the need to maintain a small device limits the ability to implement multiple antennas with uncorrelated spatial paths. However, the base station does not have such limitations and can house multiple antennas spaced sufficiently far apart to meet the requirements for uncorrelated fading paths, which are typically in the region of $10\lambda$, where $\lambda$ is the wavelength of the carrier. For example, given a typical C band communications system operating at 5 GHz with $\lambda = 60 \text{ mm}$, each antenna has to be spaced at least 60 cm apart. This is easily achieved at a base station but is not practical in a portable device.

The scope of this thesis is restricted to the performance evaluation to MISO systems with four transmit antennas and one receive antenna, thereby enabling up to a maximum diversity order of four. Three distinct codes, two of which are orthogonal and one quasi-orthogonal, are studied with three different modulation schemes. The three codes are a rate 1 Alamouti 2x diversity code, a rate ½ orthogonal 4x diversity code, and a rate 1 quasi-orthogonal 4x diversity code. The modulation schemes used are QPSK, 16-

QAM and 64-QAM. BPSK has the same bit error performance as QPSK and is not explicitly simulated. All cases assume a quasi-static flat fading environment where the channel taps remain constant for the duration of the code block, i.e., for four sample durations in the case of a 4x4 code.

## B. ORTHOGONAL SPACE-TIME BLOCK CODES

The term orthogonal space-time code borrows the mathematical concept of an orthogonal matrix. With reference to [5], the definition of an orthogonal code is given as follows:

*Definition 1: An orthogonal space-time block code with a code matrix $\boldsymbol{G}$ of dimension $T \times n$, where $T$ is the number of time slots and $n$ the number of transmit antenna has a Gramian matrix $\boldsymbol{G}^{\mathcal{H}}\boldsymbol{G}$ such that $\boldsymbol{G}^{\mathcal{H}}\boldsymbol{G} = \left( |s_1|^2 + |s_2|^2 + \cdots + |s_k|^2 \right) I$ where $s_i$ are the entries in the code matrix $\boldsymbol{G}$ corresponding to the symbols being transmitted. Such a code is said to have code rate of k/T.*

Orthogonal codes have the important property that the transmit sequences are orthogonal to one another. This implies that all the transmit symbols can be decoupled from one another. This results in a simple maximum likelihood (ML) decoder that allows the use of independent decision statistics for every symbol transmitted. The two orthogonal codes presented below illustrate this.

### 1. Rate 1 Orthogonal 2x Diversity Code (Alamouti Code)

The Alamouti code was the first space-time block code that achieved full spatial diversity while maintaining orthogonality between symbols, which leads to a simple decoder implementation. It is also the only code to achieve full orthogonal diversity with a code rate of 1. That is, one symbol is transmitted per time slot. Denoting $\boldsymbol{G}$ as the code matrix, where the row index corresponds to the time index and the column index corresponds to the antenna, we have

$$G = \begin{bmatrix} s_1 & s_2 \\ -s_2^* & s_1^* \end{bmatrix} \begin{matrix} \leftarrow \text{ time 1} \\ \leftarrow \text{ time 2} \end{matrix}$$

$$\begin{matrix} \uparrow & \uparrow \\ \text{ant 1} & \text{ant 2} \end{matrix}$$

(3.1)

where $s_1$ and $s_2$ are the modulated symbols and $a^*$ denotes the complex conjugate of $a$. Denoting $h_i = |h_i| e^{j\theta_i}, i = 1, 2$ where $h_i$ is the channel tap corresponding to transmit antenna $i$ to the receiving antenna, we have

$$r = \sqrt{\frac{\rho}{n}} Gh + n$$

$$\begin{bmatrix} r_1 \\ r_2 \end{bmatrix} = \sqrt{\frac{\rho}{2}} \begin{bmatrix} s_1 & s_2 \\ -s_2^* & s_1^* \end{bmatrix} \begin{bmatrix} h_1 \\ h_2 \end{bmatrix} + \begin{bmatrix} n_1 \\ n_2 \end{bmatrix}$$

(3.2)

$$= \sqrt{\frac{\rho}{2}} \begin{bmatrix} h_1 s_1 + h_2 s_2 + n_1 \\ -h_1 s_2^* + h_2 s_1^* + n_2 \end{bmatrix}$$

where $r_1$ and $r_2$ denote the received vector at the receiver at time slot 1 and 2, $\rho$ denotes the signal-to-noise ratio, and $n_i$ denotes the normalized noise vector with variance 2. The factor of $n = 2$ in $\sqrt{\frac{\rho}{n}}$ represents the normalizing of the transmitter power across two antennas.

If the received vector is remapped by taking the complex conjugate of $r_2$ and denoting it as vector $Y$, the system model can be expressed as

$$\begin{bmatrix} r_1 \\ r_2^* \end{bmatrix} = \sqrt{\frac{\rho}{2}} \begin{bmatrix} h_1 s_1 + h_2 s_2 + n_1 \\ h_2^* s_1 - h_1^* s_2 + n_2^* \end{bmatrix}$$

$$Y = \sqrt{\frac{\rho}{2}} \begin{bmatrix} h_1 & h_2 \\ h_2^* & -h_1^* \end{bmatrix} \begin{bmatrix} s_1 \\ s_2 \end{bmatrix} + \begin{bmatrix} n_1 \\ n_2^* \end{bmatrix}$$

(3.3)

$$Y = \sqrt{\frac{\rho}{2}} Hs + N.$$

Note that the matrix $H$ is orthogonal and, therefore, $H^{\mathcal{H}} H = \|h\|^2 I$ where $H^{\mathcal{H}}$ denotes the Hermitian transpose of $H$ (i.e., the complex conjugate transpose of $H$) and

15

$\|h\|^2 = |h_1|^2 + |h_2|^2$. Assuming perfect channel state information (CSI), where $h$ is precisely known and defining $\tilde{s}_1$ and $\tilde{s}_2$ as the decision statistics, we have the normalized decision statistics

$$
\begin{aligned}
\tilde{s} &= \begin{bmatrix} \tilde{s}_1 \\ \tilde{s}_2 \end{bmatrix} \\
&= \frac{1}{\|h\|^2} H^{\mathcal{H}} Y \\
&= \frac{1}{\|h\|^2} \sqrt{\frac{\rho}{2}} H^{\mathcal{H}} Hs + \frac{1}{\|h\|^2} H^{\mathcal{H}} \begin{bmatrix} n_1 \\ n_2^* \end{bmatrix} \\
&= \sqrt{\frac{\rho}{2}} s + \frac{1}{\|h\|^2} \begin{bmatrix} h_1^* n_1 + h_2 n_2^* \\ h_2^* n_1 - h_1 n_2^* \end{bmatrix}.
\end{aligned}
\tag{3.4}
$$

Using maximum likelihood (ML) decoding, we obtain the symbol estimates

$$
\hat{s}_1 = \arg\min_{\hat{s}_1 \in S} d^2(\tilde{s}_1, \hat{s}_1)
\tag{3.5}
$$

$$
\hat{s}_2 = \arg\min_{\hat{s}_2 \in S} d^2(\tilde{s}_2, \hat{s}_2)
\tag{3.6}
$$

where $\arg\min_{x \in S} f(x)$ denotes the global minimum of $f(x)$ for $x \in S$ and $d(a,b)$ is the Euclidean distance between $a$ and $b$ and can be calculated using the matrix norm function given by $d(a,b) = \|a - b\|$. The set $S$ is the complete set of constellation points for the particular modulation scheme in use (e.g., 16-QAM). Therefore, to implement (3.5) and (3.6), the ML decoder has to substitute all possible constellation points into $\hat{s}_i$, calculate the Euclidean distance between $\hat{s}_i$ and $\tilde{s}_i$, and choose the constellation point with the minimum distance as the estimate of $s_i$.

## 2.    Rate ½ Orthogonal 4x Diversity Code

It has been proven that no orthogonal codes beyond diversity two can achieve full unity rate for a complex constellation ([5]). However, it is possible to construct any arbitrary rate ½ code for diversity beyond two. To evaluate the performance of a rate ½ orthogonal code, an example is taken from [1] with the code matrix given as

$$G = \begin{bmatrix} s_1 & s_2 & s_3 & s_4 \\ -s_2 & s_1 & -s_4 & s_3 \\ -s_3 & s_4 & s_1 & -s_2 \\ -s_4 & -s_3 & s_2 & s_1 \\ s_1^* & s_2^* & s_3^* & s_4^* \\ -s_2^* & s_1^* & -s_4^* & s_3^* \\ -s_3^* & s_4^* & s_1^* & -s_2^* \\ -s_4^* & -s_3^* & s_2^* & s_1^* \end{bmatrix}. \tag{3.7}$$

The system model is given by $Y = \sqrt{\dfrac{\rho}{n}} Hs + N$, where $n = 4$ represents the normalization of the power split across four antennas, and $N$ is the normalized noise vector with variance of two. By performing the same mapping on the received vector as for the Alamouti code per equation (3.3), we derive the matrix $H$ as

$$H = \begin{bmatrix} h_1 & h_2 & h_3 & h_4 \\ h_2 & -h_1 & h_4 & -h_3 \\ h_3 & -h_4 & -h_1 & h_2 \\ h_4 & h_3 & -h_2 & -h_1 \\ h_1^* & h_2^* & h_3^* & h_4^* \\ h_2^* & -h_1^* & h_4^* & -h_3^* \\ h_3^* & -h_4^* & -h_1^* & h_2^* \\ h_4^* & h_3^* & -h_2^* & -h_1^* \end{bmatrix}. \tag{3.8}$$

The detailed derivation for $H$ is given in Appendix A. Note that $H^H H = 2\|h\|^2 I$, and, therefore, $H$ is an orthogonal matrix. The normalized decision statistics are given by

17

$$\tilde{s} = \begin{bmatrix} \tilde{s}_1 & \tilde{s}_2 & \tilde{s}_3 & \tilde{s}_4 \end{bmatrix}^T$$

$$= \frac{1}{2\|h\|^2} H^{\mathcal{H}} Y$$

$$= \frac{1}{2\|h\|^2} \sqrt{\frac{\rho}{4}} H^{\mathcal{H}} H.s + \frac{1}{2\|h\|^2} H^{\mathcal{H}} \begin{bmatrix} n_1 & n_2 & n_3 & n_4 & n_5^* & n_6^* & n_7^* & n_8^* \end{bmatrix}^T \tag{3.9}$$

$$= \sqrt{\frac{\rho}{4}} s + \frac{1}{2\|h\|^2} \begin{bmatrix} n_1 h_1^* + n_2 h_2^* + h_1 n_5^* + n_3 h_3^* + h_2 n_6^* + n_4 h_4^* + h_3 n_7^* + h_4 n_8^* \\ n_1 h_2^* - n_2 h_1^* - h_1 n_6^* + h_2 n_5^* - n_3 h_4^* + n_4 h_3^* + h_3 n_8^* - h_4 n_7^* \\ n_1 h_3^* - n_3 h_1^* + n_2 h_4^* - n_4 h_2^* - h_1 n_7^* + h_3 n_5^* - h_2 n_8^* + h_4 n_6^* \\ n_1 h_4^* - n_2 h_3^* + n_3 h_2^* - n_4 h_1^* - h_1 n_8^* + h_2 n_7^* - h_3 n_6^* + h_4 n_5^* \end{bmatrix}.$$

Using maximum likelihood (ML) decoding, we obtain the symbol estimates

$$\hat{s}_1 = \arg\min_{\hat{s}_1 \in S} d^2(\tilde{s}_1, \hat{s}_1) \tag{3.10}$$

$$\hat{s}_2 = \arg\min_{\hat{s}_2 \in S} d^2(\tilde{s}_2, \hat{s}_2) \tag{3.11}$$

$$\hat{s}_3 = \arg\min_{\hat{s}_3 \in S} d^2(\tilde{s}_3, \hat{s}_3) \tag{3.12}$$

$$\hat{s}_4 = \arg\min_{\hat{s}_4 \in S} d^2(\tilde{s}_4, \hat{s}_4) \tag{3.13}$$

## C.    QUASI-ORTHOGONAL SPACE-TIME CODE

There exists another class of codes known as the quasi-orthogonal space-time block codes ([6] – [11]), sometimes abbreviated as QO-STBC. As described in Section III.B.2, no orthogonal codes with full unity rate exist beyond a diversity order of two when using any modulation schemes with a complex constellation. Therefore, the main motivation behind the research on QO-STBC is to exploit higher orders of diversity beyond two while maintaining full unity code rate.

Surprisingly, there does not seem to exist an official definition of quasi-orthogonal codes based on existing literature; although, there is an implicit understanding that QO-STBC are STBCs that have $H$ matrices that are not orthogonal, i.e., $H^{\mathcal{H}} H \neq \|h\|^2 I$. From the proposed definition in [6], we define a QO-STBC as follows:

***Definition 2**: A QO-STBC of dimension $N \times N$ has a **H** matrix such that $\mathbf{H}^{\mathcal{H}}\mathbf{H}$ is a sparse matrix with $\|h\|^2$ on its main diagonal, at least $N^2/2$ zero entries on its off-diagonal, and the magnitude for the rest of the entries being some value bounded by $\pm \|h\|^2$.*

This definition of a QO-STBC will become clear in an example in the next section.

### 1. Rate 1 Quasi-Orthogonal (QO) 4x Diversity Code

Given the QO-STBC in [8], the code matrix is

$$\mathbf{G} = \begin{bmatrix} s_1 & s_2 & s_3 & s_4 \\ s_2^* & -s_1^* & s_4^* & -s_3^* \\ s_3 & -s_4 & -s_1 & s_2 \\ s_4^* & s_3^* & -s_2^* & -s_1^* \end{bmatrix}. \tag{3.14}$$

Given the same mapping sequence that used for the Alamouti code, the system model is given as $\mathbf{Y} = \sqrt{\dfrac{\rho}{4}}\mathbf{H}s + \mathbf{N}$, where **H** is given by

$$\mathbf{H} = \begin{bmatrix} h_1 & h_2 & h_3 & h_4 \\ -h_2^* & h_1^* & -h_4^* & h_3^* \\ -h_3 & h_4 & h_1 & -h_2 \\ -h_4^* & -h_3^* & h_2^* & h_1^* \end{bmatrix}. \tag{3.15}$$

The detailed derivation for **H** can be found in Appendix A. Note that **H** is not orthogonal as

$$\mathbf{H}^{\mathcal{H}}\mathbf{H} = \begin{bmatrix} \|\mathbf{h}\|^2 & 0 & a & 0 \\ 0 & \|\mathbf{h}\|^2 & 0 & -a \\ -a & 0 & \|\mathbf{h}\|^2 & 0 \\ 0 & a & 0 & \|\mathbf{h}\|^2 \end{bmatrix} \tag{3.16}$$

where $a = h_3 h_1^* - h_1 h_3^* + h_2 h_4^* - h_4 h_2^* = 2j \operatorname{Im}(h_3 h_1^* + h_2 h_4^*)$ and $j$ denotes the imaginary number $j = \sqrt{-1}$. From (3.16), it is clear that $s_1$ is orthogonal to $s_2$ and $s_4$ but not $s_3$

19

(columns 2 and 4 on row 1 are zero but column 3 is non-zero). Similarly, $s_2$ is orthogonal to $s_1$ and $s_3$ but not $s_4$ (columns 1 and 3 on row 2 are zero but column 4 is non-zero). This implies that the symbol pair $(s_1, s_3)$ is orthogonal to $(s_2, s_4)$, but each of the symbols within the symbol pair contributes an interference factor of $\pm a$ to each other. The interference term $a = 2j \operatorname{Im}(h_3 h_1^* + h_2 h_4^*)$ is bounded by $\pm j \|h\|^2$. An equivalent way of saying this is that $a / \|h\|^2$ is bounded by $\pm j$. These bounds become intuitively clear by letting $|h_i| = 1$ for all channel taps; then $a / \|h\|^2 = 2j(1+1)/4 = j$. Also note that the matrix in (3.16) satisfies Definition 2 as there is a sparse matrix with $\|h\|^2$ on its diagonal, eight zero entries and four non-zero entries bounded by $\pm j \|h\|^2$ in the off-diagonal.

From the above analysis, it is clear that the single-symbol ML decoding scheme used in the orthogonal codes will not work for a quasi-orthogonal code. However, a *pairwise* ML decoding for the symbol pair $(s_1, s_3)$ and $(s_2, s_4)$ can be done separately. This is still simpler than decoding all four symbols simultaneously. This increases the decoding complexity from $\mathcal{O}(m)$ to $\mathcal{O}(m^2)$, where $m$ is the number of constellation points, as the pairwise ML decoder needs to try every possible *pair* of symbols.

Therefore, the H matrix is split into two separate parts as follows:

$$\boldsymbol{H}_{13} = \begin{bmatrix} h_1 & h_3 \\ -h_2^* & -h_4^* \\ -h_3 & h_1 \\ -h_4^* & h_2^* \end{bmatrix} \qquad (3.17)$$

$$\boldsymbol{H}_{24} = \begin{bmatrix} h_2 & h_4 \\ h_1^* & h_3^* \\ h_4 & -h_2 \\ -h_3^* & h_1^* \end{bmatrix} \qquad (3.18)$$

20

These matrices are derived from the original $H$ matrix by taking the first and third column for $H_{13}$ and 2nd and 4th column for $H_{24}$, respectively. The decoder can then perform the pairwise ML decoding as follows:

$$\{\hat{s}_1, \hat{s}_3\} = \arg \min_{\{\hat{s}_1, \hat{s}_3\} \in S} \left\| Y - \sqrt{\frac{\rho}{4}} H_{13} \begin{bmatrix} \hat{s}_1 \\ \hat{s}_3 \end{bmatrix} \right\|^2 \tag{3.19}$$

$$\{\hat{s}_2, \hat{s}_4\} = \arg \min_{\{\hat{s}_2, \hat{s}_4\} \in S} \left\| Y - \sqrt{\frac{\rho}{4}} H_{24} \begin{bmatrix} \hat{s}_2 \\ \hat{s}_4 \end{bmatrix} \right\|^2 \tag{3.20}$$

To implement (3.19), the ML decoder needs to substitute all possible permutations of $\{\hat{s}_1, \hat{s}_3\}$ and calculate the minimum matrix norm as per the equations. The number of permutations will be $m^2$ for pairwise ML decoding instead of $m$ for a single symbol ML decoding. The same can be done for (3.20).

## 2.    Constellation Rotation for QO-STBC to Achieve Full Diversity

The above QO-STBC scheme does not achieve full diversity if the symbol pairs are chosen from the same constellation ([8] – [11]). In the high SNR region, where wireless links typically operate, high order diversity has been shown to be much more important to the BER performance of the wireless link as the gradient of the BER versus SNR curves, which are steeper with high orders of diversity ([3], [9], [13], [14]). Several references ([8] – [11]) propose that the constellation for one set of the symbols be chosen from a rotated copy of the other symbol set in order to maximize diversity. The optimum angle to rotate the constellation depends on the actual constellation being used.

From [9] and [12] and given two distinct codeword matrices $C$ and $\tilde{C}$ such that $\{C, \tilde{C}\} \in G$, where $G$ is a valid QO-STBC code matrix, the pairwise error probability (PEP) $P(C \to \tilde{C})$ in a Rayleigh fading channel is given by

$$P\left(C \to \tilde{C}\right) \leq \frac{1}{2} \left( \prod_{i=1}^{r} \lambda_i \right)^{-m} \left( \frac{\rho}{4n} \right)^{-rm} \tag{3.21}$$

21

where $\lambda_i$ are the non-zero eigenvalues of the matrix $A$ given by $A = (C - \tilde{C})^{\mathcal{H}}(C - \tilde{C})$, $r$ is the rank of the matrix $B$ given by $B = (C - \tilde{C})$, $\rho$ is the SNR, $n$ is the number of transmit antenna, and $m$ is the number of receive antenna. Furthermore, (3.21) is only valid if $B$ is of full rank, i.e., for every $C \neq \tilde{C}$, the hyperpoint spanned by $(C - \tilde{C})$ is a unique point within the entire hyperspace of all possible permutations of $(C - \tilde{C})$. In other words, no two distinct $\{C, \tilde{C}\}$ codeword pairs can result in the same received signal $Y$. Since the purpose is to design QO-STBC that are of full diversity, $B$ must be of full rank.

From (3.21), it is clear that in order to minimize the PEP of the code matrix $G$, the rank of matrix $B$ and the product of the eigenvalues of $A$ must be maximized. Therefore, the well-known *rank and determinant criteria* in [12] are as follows:

*Rank Criterion* (also called the Diversity Criterion) states that the minimum rank of the code difference matrix $B\big|_{C \neq \tilde{C}} = (C - \tilde{C})$ must be as large as possible in order to achieve maximum diversity. This implies that $B$ must be of full-rank and, thus, invertible.

*Determinant Criterion* (also called the Product Criterion) states that the product of the non-zero eigenvalues of the matrix $A = B^{\mathcal{H}}B$ must be as large as possible to achieve the maximum coding gain. Note that if $B$ is of full rank, then $A$ will be of full rank as well, and the product of the eigenvalues $\prod_{i=1}^{r} \lambda_i$ of $A$ is simply the determinant of $A$.

If $A$ and $B$ are of full rank, then $\prod_{i=1}^{r} \lambda_i = \det(A)$. Substituting this into (3.21), we get

$$P\left(C \to \tilde{C}\right) \le \frac{1}{2}\left(\det(A)\right)^{-m}\left(\frac{\rho}{4n}\right)^{-rm}$$

$$= \frac{1}{2}\left(\left(\det(A)\right)^{1/r}\frac{\rho}{4n}\right)^{-rm}$$

$$= \frac{1}{2}\left(\frac{\left(\det(A)\right)^{1/r}}{4n}\rho\right)^{-rm} \tag{3.22}$$

$$= \frac{1}{2}\left(\zeta^2_{\{C,\tilde{C}\}}\rho\right)^{-rm}$$

where $\zeta^2_{\{C,\tilde{C}\}} = \left(\det(A)\right)^{1/r}/4n$ is defined for a specific codeword pair $\{C,\tilde{C}\}$. Considering the PEP across all possible permutations of the codeword pair $\{C,\tilde{C}\}$, we see that the worst performance is dictated by the minimum determinant of $A$ obtained by substituting all possible permutations of $\{C,\tilde{C}\}$, i.e.,

$$\zeta^2 = \frac{1}{4n}\min_{C \ne \tilde{C}}\left|\det\left[(C - \tilde{C})^{\mathcal{H}}(C - \tilde{C})\right]\right|^{1/r}. \tag{3.23}$$

The term $\zeta$ is known as the *diversity product* and can be calculated by taking the square root of (3.23). The union bound on the PEP of the any given code $G$ is given as follows:

$$P\left(C \to \tilde{C}\right) \le \frac{1}{2}\left(\zeta^2\rho\right)^{-rm}. \tag{3.24}$$

Now, consider the QO-STBC given in (3.14) assuming that there is only one receiver antenna. As analyzed in Section III.C.1, the symbol pairs $(s_1, s_3)$ and $(s_2, s_4)$ are orthogonal to each other, but the individual symbols within the pair are not orthogonal. In order to maximize the diversity of the QO-STBC, the encoder must maximize the rank and determinant of the codeword difference matrix $(C - \tilde{C})$ of the symbol pair. This is equivalent to maximizing the diversity product given in (3.23). Since $(s_1, s_3)$ and $(s_2, s_4)$ are orthogonal to each other, the minimum achievable diversity is at least of order two since the rank of $B$ is at least two. To achieve the maximum diversity of four for the QO-STBC, the code design only needs to consider the non-orthogonal elements of the QO-

STBC, i.e., either $(s_1, s_3)$ or $(s_2, s_4)$. By considering either the symbol pair $(s_1, s_3)$ or $(s_2, s_4)$ in $G$, we can break the matrix into four different sub-matrices as follows:

$$G_{13} = \begin{bmatrix} s_1 & s_3 \\ s_3 & -s_1 \end{bmatrix} \quad G_{24} = \begin{bmatrix} s_2 & s_4 \\ -s_4 & s_2 \end{bmatrix} \quad G_{1^*3^*} = \begin{bmatrix} -s_1^* & -s_3^* \\ s_3^* & -s_1^* \end{bmatrix} \quad G_{2^*4^*} = \begin{bmatrix} s_2^* & s_4^* \\ s_4^* & -s_2^* \end{bmatrix}. \quad (3.25)$$

The above non-orthogonal sub-matrices are derived from $G$ by simply deleting the appropriate rows and columns such that we are left with either $(s_1, s_3)$ or $(s_2, s_4)$. The ranks of these matrices are either zero or two depending on the actual symbols being transmitted. Therefore, from the rank and determinant criterion, the objective of maximizing the diversity in $G$ is equivalent to maximizing the diversity product of its sub-matrices. In addition, it does not matter which of the sub-matrices is used to evaluate the diversity product as $\det(G_{13}^{\mathcal{H}} G_{13}) = \det(G_{1^*3^*}^{\mathcal{H}} G_{1^*3^*}) = \det(G_{24}^{\mathcal{H}} G_{24}) = \det(G_{2^*4^*}^{\mathcal{H}} G_{2^*4^*})$ if the same symbol pairs are sent using any of the four sub-matrices. Since all possible permutations of the symbol pairs will be evaluated, the diversity product for all four sub-matrices must be the same as well.

Consider the sub-matrix $G_{13}$, the determinant of its Gramian matrix $G_{13}^{\mathcal{H}} G_{13}$ expressed as

$$\det\left(G_{13}^{\mathcal{H}} G_{13}\right) = \left(s_1^2 + s_3^2\right)\left((s_1^*)^2 + (s_3^*)^2\right). \quad (3.26)$$

Let $C_{13}$ and $\tilde{C}_{13}$ be two distinct code words of the sub-matrix $G_{13}$, and define the Gramian of the code difference matrix $A_{13} = \left(C_{13} - \tilde{C}_{13}\right)^{\mathcal{H}} \left(C_{13} - \tilde{C}_{13}\right)$. The determinant of the $A_{13}$ can be derived from (3.26) by inspection as

$$\det\left(A_{13}\right) = \left((s_1 - \tilde{s}_1)^2 + (s_3 - \tilde{s}_3)^2\right)\left((s_1^* - \tilde{s}_1^*)^2 + (s_3^* - \tilde{s}_3^*)^2\right). \quad (3.27)$$

Note that if $(s_1, \tilde{s}_1)$ and $(s_3, \tilde{s}_3)$ are selected from the same constellation, then $\det(A_{13})$ can potentially be zero, e.g., when $(s_1 - \tilde{s}_1) = j(s_3 - \tilde{s}_3)$. The only situation where $A_{13}$ can be of full rank when $(s_1, \tilde{s}_1)$ and $(s_3, \tilde{s}_3)$ are chosen from the same constellation is when the constellation consists of only one basis vector, e.g., in ASK where constellation points are purely real. Therefore, in order to achieve full diversity, $(s_1, \tilde{s}_1)$

24

must be chosen from a different constellation from $(s_3, \tilde{s}_3)$ to eliminate the possibility of $\det(A_{13})$ being zero.

Let $\mathcal{A}$ and $\mathcal{B}$ be the signal constellations for $(s_1, \tilde{s}_1)$ and $(s_3, \tilde{s}_3)$, respectively, and $\mathcal{B}$ is a rotated version of $\mathcal{A}$ given by $\mathcal{B} = \mathcal{A}e^{j\theta}$. With a properly chosen rotation angle, $A_{13}$ can be of full rank, and the problem now is to maximize the diversity product in accordance with the determinant criterion. Combining (3.23) with (3.27), we get

$$\zeta^2 = \frac{1}{4n} \min_{c \neq \tilde{c}} \left| \left( (s_1 - \tilde{s}_1)^2 + (s_3 - \tilde{s}_3)^2 \right) \left( (s_1^* - \tilde{s}_1^*)^2 + (s_3^* - \tilde{s}_3^*)^2 \right) \right|^{1/r} \qquad (3.28)$$

where $(s_1, s_3) \in C$ and $(\tilde{s}_1, \tilde{s}_3) \in \tilde{C}$ and $(s_1, \tilde{s}_1) \in \mathcal{A}$ and $(s_3, \tilde{s}_3) \in \mathcal{B}$. Given that $n = 4$ and $r = 2$ for our QO-STBC and taking the square root of (3.28) produces

$$\zeta = \frac{1}{4} \min_{c \neq \tilde{c}} \left| \left( (s_1 - \tilde{s}_1)^2 + (s_3 - \tilde{s}_3)^2 \right) \right|^{1/2}. \qquad (3.29)$$

With (3.29), a numerical search for the rotation angle for constellation $\mathcal{B}$ can be performed to maximize $\zeta$. Reference [9] provides an analytical proof that the optimal rotation angle for rectangular constellations is 45°. This claim is validated in Chapter IV.

THIS PAGE INTENTIONALLY LEFT BLANK

# IV. PERFORMANCE EVALUATION AND ANALYSIS FOR SPACE-TIME CODES

The performance of various space-time codes covered in Chapter III are presented in this chapter. Analysis of the results is also presented where applicable.

## A. PERFORMANCE EVALUATION OF QUASI-ORTHOGONAL SPACE-TIME BLOCK CODES

We begin with the evaluation of the optimum rotation angle for three different modulation schemes (QPSK, 16-QAM and 64-QAM) as well as the simulation results using various angles of constellation rotation. The constellation maps used for the modulation, based on the IEEE 802.16-2009, are located on page 631 of [23].

### 1. Evaluation of Optimal Angle of Rotation

From (3.29), the diversity product is plotted against rotation angle for all modulation schemes as shown in Figure 5.

There are several interesting features of the diversity product plot. Firstly, it validates that 45° is indeed an optimum rotation angle for all three modulation schemes (which all have a rectangular constellation) as mentioned in [9]. However, there also exist several ranges of angles where diversity is maximum, all of which are as tabulated in Table 2. In addition, the plot of the diversity product, with respect to the rotation angle, is clearly symmetrical about the 45° line, as can be seen in Figure 5.

Table 2.     Maximum diversity products and corresponding rotation angles.

|  | Maximum diversity product, $\zeta_{max}$ | Valid range of angles for $\zeta_{max}$ |
|---|---|---|
| QPSK | 0.3536 | 30° − 60° |
| 16-QAM | 0.1581 | 30° − 31.13°, 42.61° − 47.39°, 58.87° − 60° |
| 64-QAM | 0.0772 | 30° − 30.07°, 30.96° − 31.13°, 42.61°, 44.59° − 45.41°, 47.39°, 58.87° − 59.04°, 59.93° − 60° |
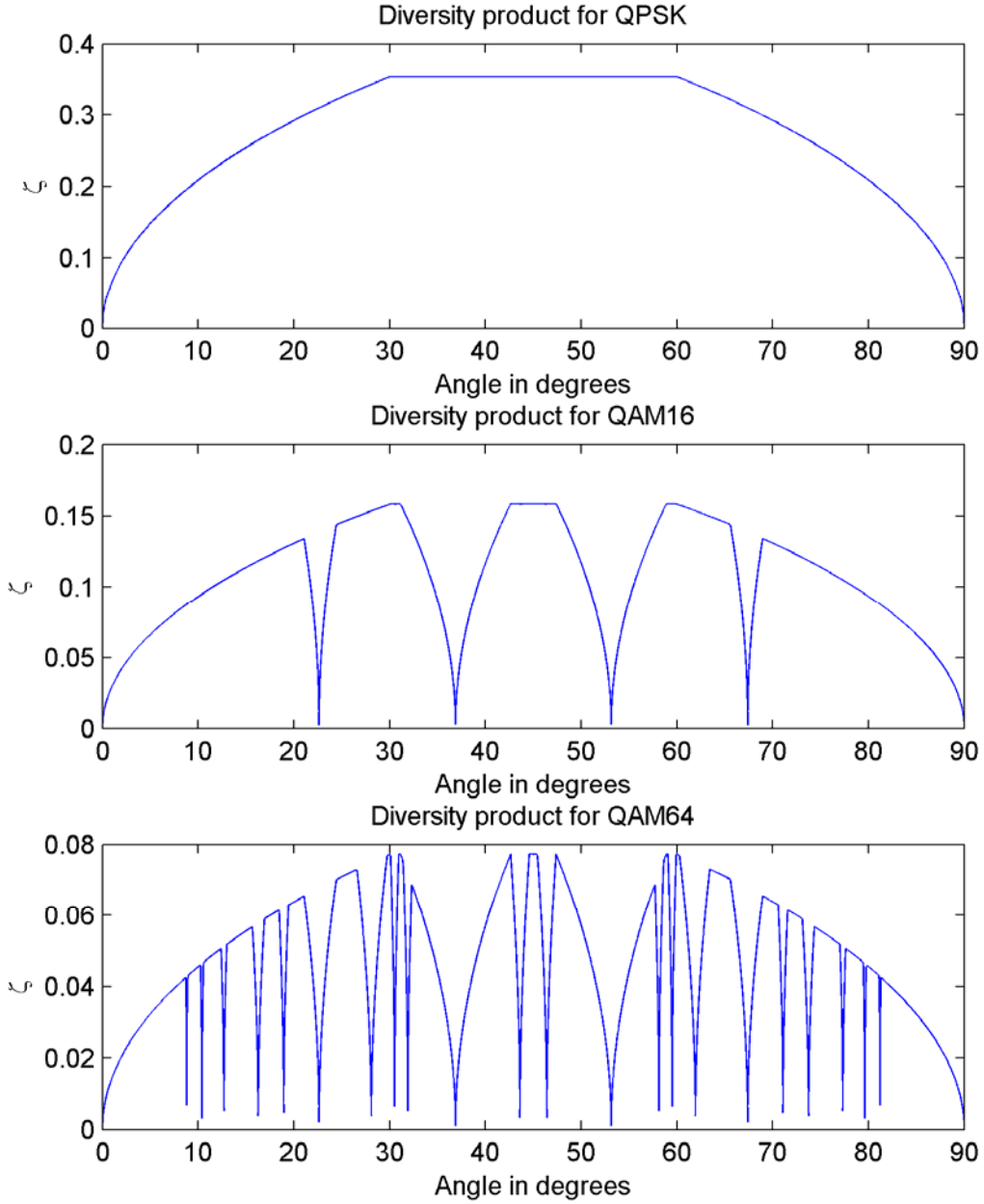
Figure 5.        Diversity product against angle for three different modulation schemes.

### 2.        Simulation and Analysis for BER of QO-STBC

To evaluate the bit error rate (BER) performance for the QO-STBC given in Section III.C.1, four different angles to rotate the constellation for symbols $s_3$ and $s_4$ for each of the modulation schemes are chosen. Three of the angles chosen are fixed at 0°, 13.28° and 45° to represent the range of possible diversity, from the worst to the best. A

custom angle other than 45° was also chosen to test the ability to reach maximum diversity at other angles and their relationship with the diversity product. The chosen angles and their diversity product are shown in Table 3.

Table 3.    Chosen rotation angles and their corresponding diversity product.

| | Diversity Product, $\zeta$ | | | |
|---|---|---|---|---|
| Rotation angle | 0° | 13.28° | 45° | Custom angle |
| QPSK | 0 | 0.2397 | 0.3536 | 0.3536 (Angle: 34.35°) |
| 16-QAM | 0 | 0.1072 | 0.1581 | 0.1581 (Angle: 30.96°) |
| 64-QAM | 0 | 0.0523 | 0.0772 | 0.0419 (Angle: 59.36°) |

With each of the modulation schemes, simulations were done using Matlab to test the effects of the diversity scheme with various angles of rotation across a range of $E_b / N_0$, and the results are shown in Figure 6 and Figure 7.

For angles 0°, 13.28° and 45°, the behavior across all three modulations is the same, where 0° exhibited the worst BER performance with a diversity order of 2, 45° exhibited the best BER performance with a diversity order of 4, and 13.28° had a BER performance between diversity two and four. This is as predicted by the diversity product as it increases from 0° to 13.28° to 45°, as seen in Table 3 and Figure 5.

For QPSK and 16-QAM, the custom angle chosen has a diversity product that is the maximum for the corresponding modulation scheme, i.e., same $\zeta$ as that of 45°. From Figure 6, we can see that its BER performance is the same as that of 45°. This establishes that 45° is indeed not the only optimum point in which maximum diversity is achievable.

29
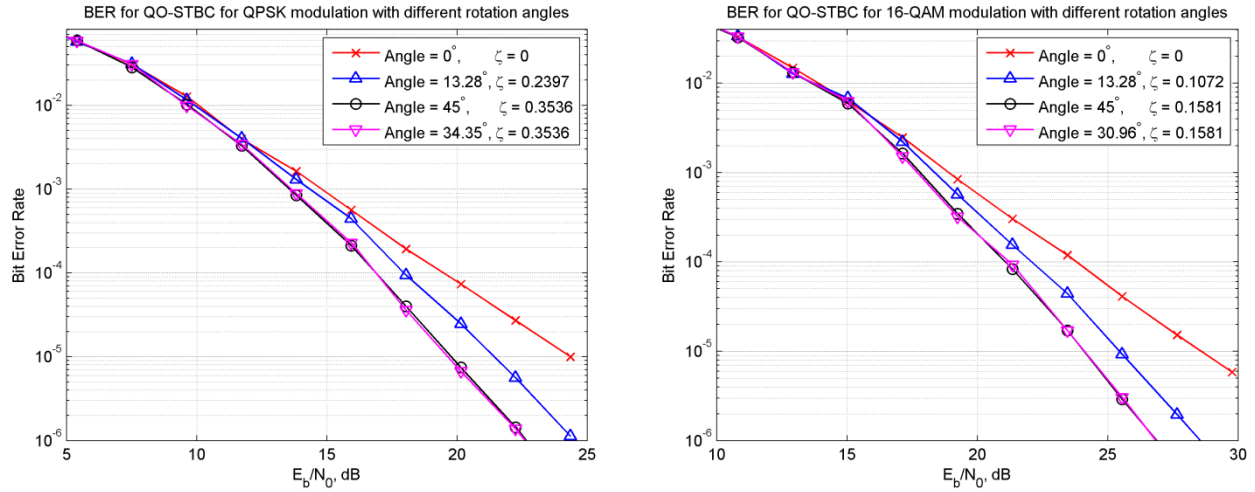
Figure 6.    BER for QO-STBC with QPSK and 16-QAM for various rotation angles.
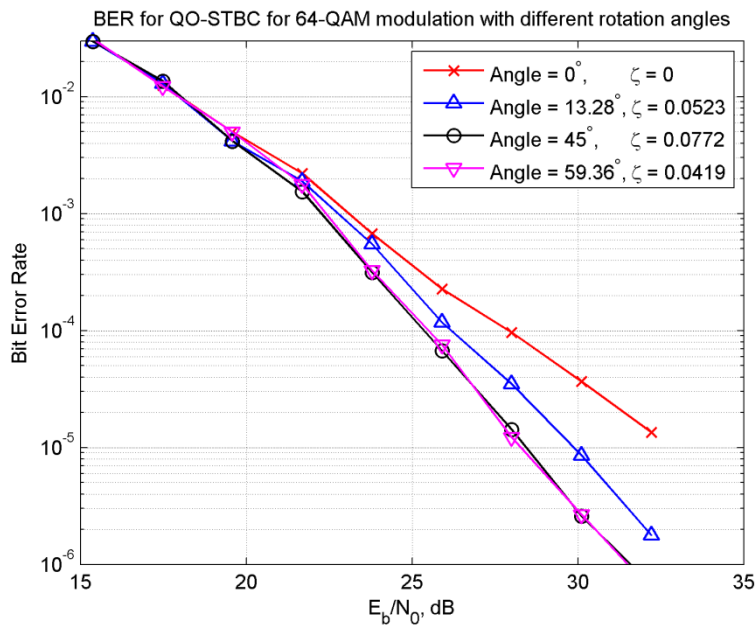


Figure 7.    BER for QO-STBC with 64-QAM for various rotation angles.

Things get more interesting with 64-QAM. As illustrated in Figure 7, the performance of the custom angle at 59.36° closely tracks that of 45° with no perceivable difference across the entire simulated $E_b / N_0$ range. However, the diversity product at 59.36° is lower than that of 45° (in fact, it is also lower than that of 13.28°). This seems

30

to imply that the minimum diversity product predicted by (3.29) is not the only factor affecting the overall performance of the QO-STBC code.

A zoomed-in view of the plot of $\zeta$ with respect to rotation angle for 64-QAM is shown in Figure 8. The angle of 59.36° lies in a narrow "valley" between 59° and 60°, which both have maximum diversity product (refer to Table 2 on the range of angles with maximum diversity and Figure 5 for how $\zeta$ varies with angle across the entire range of 0° to 90° rotation).
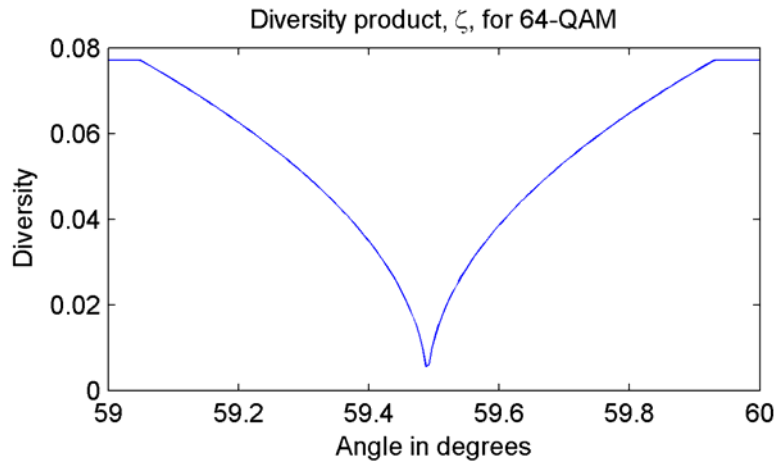


Figure 8.    Zoomed in view of $\zeta$ for 64-QAM from 59° to 60°.

To further explore this phenomenon, a computer numerical search was performed to determine the rotation angle of the valley point. It was found that the angle of $\tan^{-1}(56/33) \approx 59.4897°$ gave a lowest possible $\zeta$ of $7.88 \times 10^{-9}$. Within the limits of numerical rounding error due to the limited precision of the computer, it can be considered that the calculated $\zeta = 0$.

The simulation results using 64-QAM for four different angles of rotationis shown in Figure 9. Three of the chosen angles come from around the "valley region" but have different diversity products, while the 45° plot is left as a benchmark.
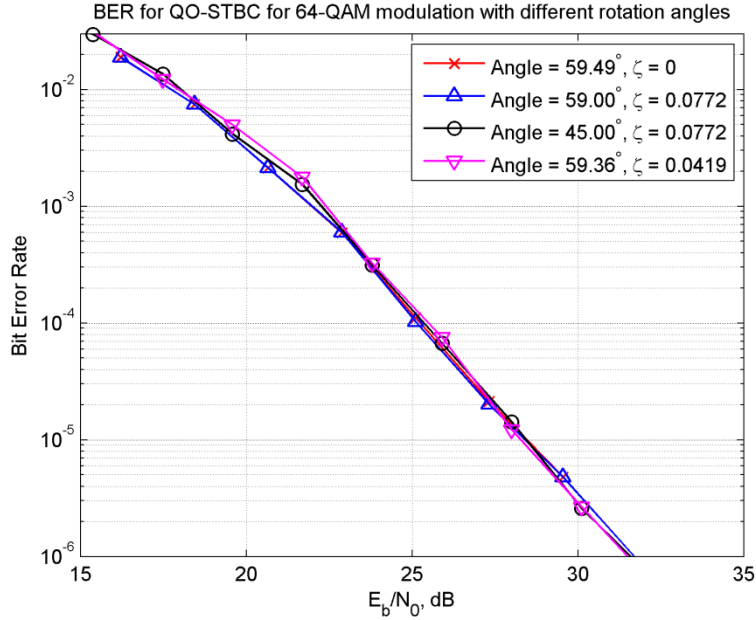
Figure 9.        BER for QO-STBC with 64-QAM using a different set of rotation angles.


It is obvious from Figure 9 that while different rotations angles have very different diversity products, the BER performance of all four curves is practically the same. In fact, for the 59.49° rotation, the QO-STBC should have been rank-deficient, and should only have achieved a performance with diversity of order two similar to that of 0° rotation. Clearly, this is not the case illustrated in Figure 9.

Therefore, we hypothesize that while the rank and determinant criteria are sufficient conditions for maximum diversity, they do not seem to be necessary.

Given that the above hypothesis is true, it then naturally follows that the union bound predicted by (3.24) will not be a useful bound since the performance of the QO-STBC is not a monotonic function of the diversity product. For example, in the above simulation, for the angle of 59.49°, the predicted error bound with $\zeta = 0$ is 0.5 across the entire $E_b / N_0$ range, which clearly is not very useful. Furthermore, this bound is the same bound for the QO-STBC with no rotation, but its BER performance is very different from that of the QO-STBC with 59.49° rotation.

## B.  PERFORMANCE EVALUATION OF SPACE-TIME BLOCK CODES

The BER of the entire family of STBC, both orthogonal and non-orthogonal, is compared in this section. The complete list of simulated STBC is shown in Table 4. For QO-STBC, the rotation angle is annotated as CR (short for Constellation Rotation), and both 0° and 45° CR are included in this section for diversity orders of two and four respectively. This allows for a comparison against full orthogonal codes with the same order of diversity. Note that the table is sorted by the diversity order and normalized bandwidth efficiency.

Table 4.    List of STBCs simulated.

| Modulation | STBC *G* matrix type and size | Code Rate | Diversity order | Normalised bandwidth efficiency |
|---|---|---|---|---|
| QPSK | Orthogonal 2×2 | 1 | 2 | 2 bps/Hz |
| QPSK | Quasi-Orthogonal 4×4 | 1 | 2 (CR = 0°) | 2 bps/Hz |
| 16-QAM | Orthogonal 2×2 | 1 | 2 | 4 bps/Hz |
| 16-QAM | Quasi-Orthogonal 4×4 | 1 | 2 (CR = 0°) | 4 bps/Hz |
| 64-QAM | Orthogonal 2×2 | 1 | 2 | 6 bps/Hz |
| 64-QAM | Quasi-Orthogonal 4×4 | 1 | 2 (CR = 0°) | 6 bps/Hz |
| QPSK | Orthogonal 8×4 | 0.5 | 4 | 1 bps/Hz |
| QPSK | Quasi-Orthogonal 4×4 | 1 | 4 (CR = 45°) | 2 bps/Hz |
| 16-QAM | Orthogonal 8×4 | 0.5 | 4 | 2 bps/Hz |
| 64-QAM | Orthogonal 8×4 | 0.5 | 4 | 3 bps/Hz |
| 16-QAM | Quasi-Orthogonal 4×4 | 1 | 4 (CR = 45°) | 4 bps/Hz |
| 64-QAM | Quasi-Orthogonal 4×4 | 1 | 4 (CR = 45°) | 6 bps/Hz |

### 1.  Diversity Order Two Comparison by Modulation Scheme

The results of the simulation of all modulation with a diversity order of two is shown in Figure 10. The curves for a flat Rayleigh fading channel with no diversity and a

AWGN channel are included for comparison. These curves approximately correspond to the bounds of performance for our Rayleigh fading simulations.
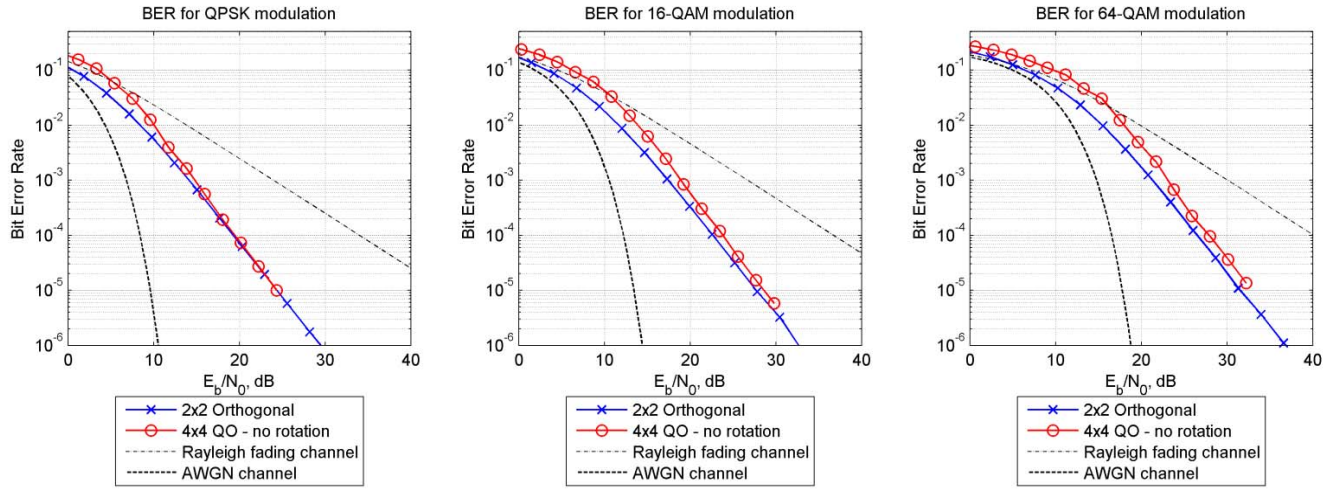


Figure 10.     BER for different modulation schemes with a diversity order of two.

From the simulation results, we have demonstrated that even a simple Alamouti 2×2 diversity scheme has the potential to significantly increase the reliability of a communications link in a fading channel. For example, there is more than 15 dB gain for the Alamouti scheme over the fading channel curve at a BER of $10^{-5}$ across all three modulation schemes. This is a significant gain considering the relative ease and low cost adding a second antenna (with its corresponding modulators, amplifiers and associated hardware) at the transmitter end. This is especially beneficial in a network environment where multiple users are connected to a single base station.

However, for the 4×4 QO-STBC with no rotation, the performance is consistently worse than the Alamouti scheme, even though it does seem to converge at the higher $E_b / N_0$ range. This clearly demonstrates the weakness of naively implementing a QO-STBC with no rotation, which only achieves a diversity order of two but requires four antennas. From both a cost and performance perspective, there is no practical reason to implement a 4×4 QO-STBC with no rotation.

## 2. Diversity Order Four Comparison by Modulation Scheme

The results of the simulation of all modulation with a diversity order of four is as shown in Figure 11.
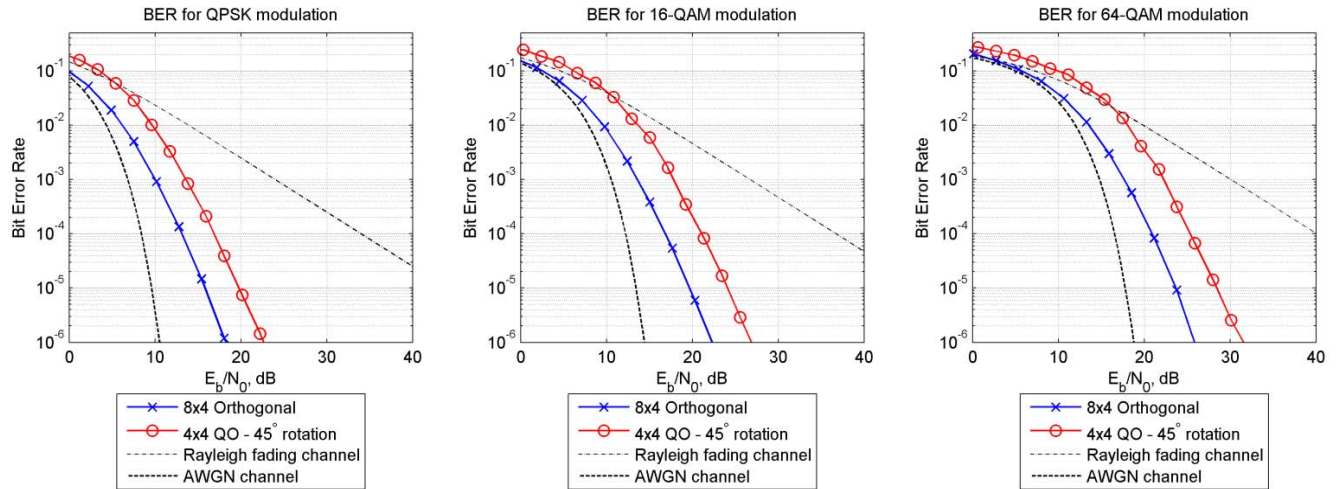


Figure 11.    BER for different modulation schemes with a diversity order of four.

It can be clearly seen from Figure 11 that a diversity order of four easily outperforms a diversity order of two, regardless of the modulation scheme used. This is especially true at higher $E_b / N_0$, where the gradient is steeper than that of second order diversity. For example, in the 8×4 orthogonal scheme, the gain is at least 25 dB at BER of $10^{-5}$ across all three modulation schemes compared to 15 dB for the Alamouti scheme.

In addition, the orthogonal scheme consistently has a higher gain over the QO scheme with all three modulations (approximately 3.8 dB for QPSK and 4.5 dB for both QAM schemes). However, this increase in BER performance comes at a cost, as the orthogonal scheme only has half of the bandwidth efficiency of the QO scheme, since its code rate is ½ (eight time slots to transmit four symbols).

## 3. Diversity Order Four Comparison by Bandwidth Efficiency

The discussion above leads to the logical comparison of the diversity performance by the bandwidth efficiency of the modulation scheme, rather than by the actual modulation. Such a comparison is shown in Figure 12.
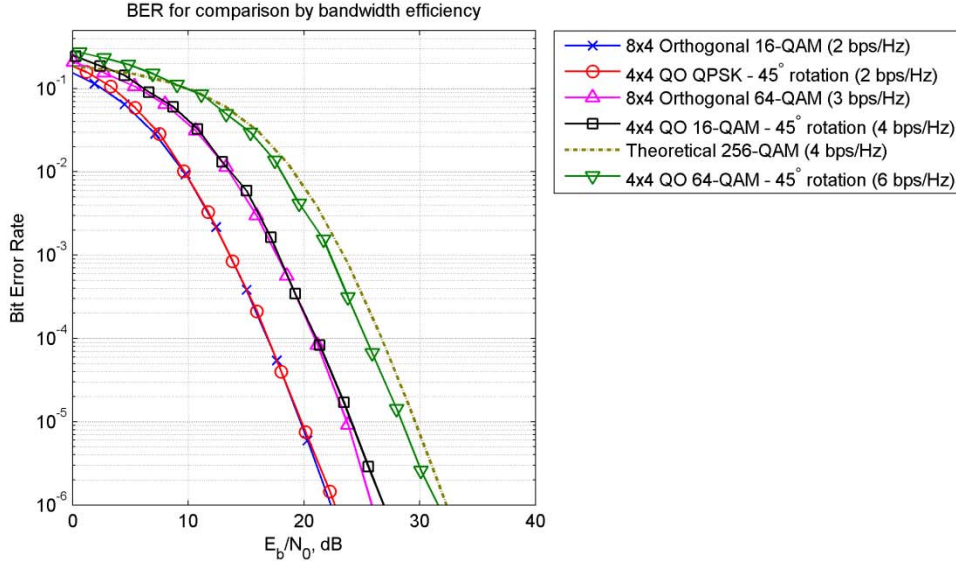
Figure 12.    BER comparison by bandwidth efficiency.

From the plots, we can see that the QO schemes start out with a poorer BER performance at the low $E_b / N_0$ region, but converge with the orthogonal scheme at the higher $E_b / N_0$ region. In addition, the BER performance corresponds very well when compared by bandwidth efficiency. Interestingly, the orthogonal 8×4 64-QAM scheme does not perform much better than the 16-QAM 4×4 QO, even though its bandwidth efficiency of 3 bps/Hz is lower than that of 16-QAM 4×4 QO with 4 bps/Hz. For the purpose of comparison, the theoretical 256-QAM with a diversity of four was also plotted. If a half-rate orthogonal code is used, the 64-QAM 4×4 QO will outperform the 256-QAM in both the BER performance and bandwidth efficiency. It should be noted that the best possible code rate achievable for orthogonal codes is ¾ for up to four antennas ([5]), even though the simulation only used code rate ½.

## C.    CONCLUSION

Based on the above results, QO-STBC with constellation rotation is a viable scheme for improving the code rate without any penalties in BER performance when compared to orthogonal STBC (O-STBC), assuming both codes have the same bandwidth

efficiency. In addition, as the modulation order increases (e.g., comparing the theoretical orthogonal 256-QAM curves with 64-QAM QO-STBC), QO-STBC also seems to outperform O-STBCs.

Another important point to note is that even when comparing the two codes at the same bandwidth efficiency, the O-STBC requires twice the time to send the same number of symbols as the QO-STBC (since its code rate is half). In a Doppler channel, where the quasi-static assumption may not be true (i.e., short coherence time), a code that requires a shorter time block (e.g., four time slots using the QO-STBC) may perform better than a code that requires a longer time block (e.g., eight times slots using the O-STBC) since the spatial channel taps are more correlated in a shorter time frame, and the channel tap estimates in the $H$ matrix are more accurate. This is another advantage of the QO-STBC over the O-STBC; it is less sensitive to the degradation introduced by a Doppler channel, as it can tolerate a shorter coherence time.

The major disadvantage with QO-STBC is the increased decoding complexity introduced by the pairwise maximum likelihood decoding. This increases the complexity from $\mathcal{O}(m)$ to $\mathcal{O}(m^2)$, where $m$ is the number of constellation points. This implies that QO-STBC may not be feasible for very high orders of modulation, as the decoding complexity increases exponentially.

THIS PAGE INTENTIONALLY LEFT BLANK

# V.    SPACE-FREQUENCY DIVERSITY

There has been considerable research into harnessing the available diversity across all domains in space, time and frequency ([13] – [17]). In the preceding chapter, we looked at harnessing spatial diversity through the proper design of space-time block codes given a quasi-static channel. It was shown that the maximum achievable diversity is limited by the number of transmit antennas (assuming that there is only one receive antenna). However, to achieve greater diversity, it is possible to harness diversity from the other two domains, namely time and frequency, in addition to spatial diversity in order to increase the diversity order at the expense of bandwidth. In this chapter, the issue of harnessing diversity from both the space and frequency domains in a quasi-static channel is explored.

Frequency diversity requires a frequency-selective channel such that the fading across different frequencies is uncorrelated. This is generally possible for mobile communications with a sufficiently large bandwidth as there usually exists a rich multipath environment for mobile devices near the ground due to large number of scatterers, especially in an urban setting.

## A.    SPACE-FREQUENCY    DIVERSITY    THROUGH    ORTHOGONAL FREQUENCY-DIVISION MULTIPLEXING (OFDM)

In recent years, orthogonal frequency-division multiplexing (OFDM) has gained widespread adoption into various technologies and standards such as Digital Audio Broadcast, Digital Video Broadcast, Wifi (802.11) and Wimax (802.16). The idea behind OFDM is to partition the allocated bandwidth into multiple overlapping narrowband signals with subcarriers on orthogonal frequencies. This implies that a high bitrate stream can be multiplexed into $N$ parallel low bitrate streams, where $N$ corresponds to the number of orthogonal subcarriers. Orthogonal frequency-division multiple access (OFDMA) takes this idea further by allowing different subcarriers to be allocated to different users, such that multiple users can share the same channel simultaneously.

Given a quasi-static frequency-selective channel with $L$ independent channel taps, $n$ transmit antenna and $m$ receive antenna, the maximum achievable diversity order is $nmL$ since the maximum rank of the codeword difference matrix $B$ is $nmL$ according to the rank criterion established in Section III.C.2 ([13], [15], [17], [18]). Given that a broadband signal is OFDM modulated such that $N \gg L$, each of the subcarriers can be viewed as a narrowband signal that experiences a quasi-static frequency-flat fading. The assumption of $N \gg L$ is generally valid for most OFDM systems since the number of subcarriers $N$ typically ranges from 64 to as high as 2,048, while the number of resolvable paths $L$ are typically modeled with no more than 20 taps (e.g., [20]). Therefore, in this context, there exists a basic equivalence between an OFDM subcarrier and an antenna, such that each subcarrier only has a single channel tap from one transmit antenna to one receive antenna.

Consider a MISO system where there are $n$ transmit antennas and one receive antenna. Using OFDM, we can transform the original broadband frequency-selective channels into $N$ parallel narrowband frequency-flat channels. This can, in turn, be seen as a single frequency-flat channel with $m$ transmit antennas and $N$ receive antennas with only a single channel tap between any transmit antenna and any receive antenna. Furthermore, with OFDMA, the modulator can select a subset of $l < L$ subcarriers for any individual user such that these $l$ subcarriers are spaced sufficiently far apart to have uncorrelated fading. This allows the MISO system to achieve maximal-ratio combining (MRC)-like diversity gains similar to a MIMO system with diversity $nl$, and this reduces the analysis to the space-time system described in Chapter III.

## B. MAXIMAL-RATIO COMBINING USING SPACE-TIME-FREQUENCY CODES

In this section, we describe a space-time-frequency (STF) block code using a MISO system with two transmit antennas, one receive antenna and using two OFDM subcarriers to achieve MRC-like diversity gains.

Consider the Alamouti space-time block code (STBC) given in (3.1). Assume that the STBC is sent across two OFDM subcarriers such that

$$G_1 = G_2 = \begin{bmatrix} s_1 & s_2 \\ -s_2^* & s_1^* \end{bmatrix}, \tag{4.1}$$

where $G_1$ and $G_2$ denote the STBCs that are sent across OFDM subcarrier 1 and 2, respectively. This forms a space-time-frequency (STF) block code with a transmit diversity of two and a frequency diversity of two as illustrated in Figure 13.
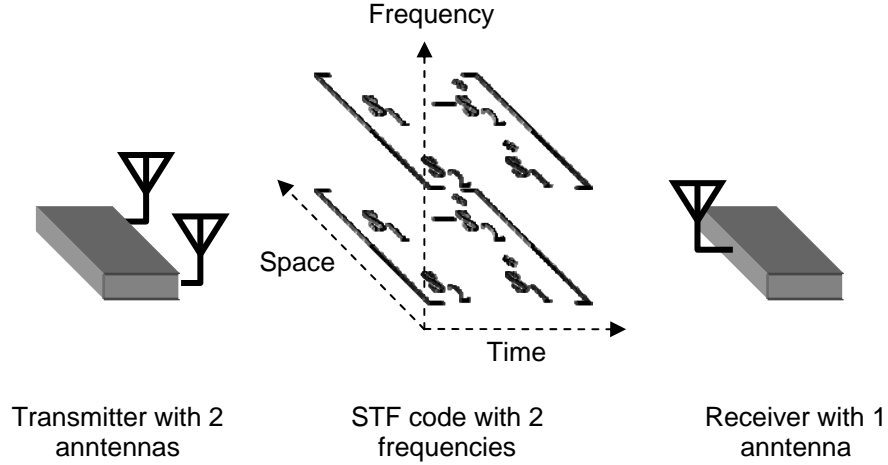


Figure 13.  Illustration of a space-time-frequency (STF) code.

Denoting the channel taps as $h_{ij}$ such that $i \in \{1,2\}$ denotes the OFDM subcarrier index, $j \in \{1,2\}$ denotes the transmit antenna, and denoting the noise vectors as $n_{ik}$ such that $i \in \{1,2\}$ denotes the OFDM subcarrier index, $k \in \{1,2\}$ denotes the time slot index, we can rewrite the received vector on the first OFDM subcarrier given in (3.3) as

$$
\begin{aligned}
Y_1 &= \sqrt{\frac{\rho}{2}} \begin{bmatrix} h_{11} & h_{12} \\ h_{12}^* & -h_{11}^* \end{bmatrix} \begin{bmatrix} s_1 \\ s_2 \end{bmatrix} + \begin{bmatrix} n_{11} \\ n_{12}^* \end{bmatrix} \\
&= \sqrt{\frac{\rho}{2}} H_1 s + N_1.
\end{aligned}
\tag{4.2}
$$

Similarly, the received vector on the second OFDM subcarrier can be rewritten as

41

$$Y_2 = \sqrt{\frac{\rho}{2}} \begin{bmatrix} h_{21} & h_{22} \\ h_{22}^* & -h_{21}^* \end{bmatrix} \begin{bmatrix} s_1 \\ s_2 \end{bmatrix} + \begin{bmatrix} n_{21} \\ n_{22}^* \end{bmatrix}$$

$$= \sqrt{\frac{\rho}{2}} H_2 s + N_2. \tag{4.3}$$

Denoting $h_1 = \begin{bmatrix} h_{11} & h_{12} \end{bmatrix}^T$, $h_2 = \begin{bmatrix} h_{21} & h_{22} \end{bmatrix}^T$, $h = \begin{bmatrix} h_1^T & h_2^T \end{bmatrix}^T$ and pre-multiplying $Y_1$

by $H_1^{\mathcal{H}}$ and $Y_2$ by $H_2^{\mathcal{H}}$ and noting that both $H_1$ and $H_2$ are orthogonal, we derive the

normalized decision statistics

$$\tilde{s} = \begin{bmatrix} \tilde{s}_1 \\ \tilde{s}_2 \end{bmatrix}$$

$$= \frac{1}{\|h_1\|^2 + \|h_2\|^2} \left( H_1^{\mathcal{H}} Y_1 + H_2^{\mathcal{H}} Y_2 \right)$$

$$= \frac{1}{\|h\|^2} \left( \sqrt{\frac{\rho}{2}} H_1^{\mathcal{H}} H_1 s + H_1^{\mathcal{H}} N_1 + \sqrt{\frac{\rho}{2}} H_2^{\mathcal{H}} H_2 s + H_2^{\mathcal{H}} N_2 \right) \tag{4.4}$$

$$= \frac{1}{\|h\|^2} \left( \sqrt{\frac{\rho}{2}} \left( \|h_1\|^2 + \|h_2\|^2 \right) s + H_1^{\mathcal{H}} N_1 + H_2^{\mathcal{H}} N_2 \right)$$

$$= \sqrt{\frac{\rho}{2}} s + \frac{1}{\|h\|^2} \begin{bmatrix} h_{11}^* n_{11} + h_{12} n_{12}^* + h_{21}^* n_{21} + h_{22} n_{22}^* \\ h_{12}^* n_{11} - h_{11} n_{12}^* + h_{22}^* n_{21} - h_{21} n_{22}^* \end{bmatrix}.$$

Using maximum-likelihood (ML) decoding, we obtain the symbol estimates

$$\hat{s}_1 = \arg \min_{\hat{s}_1 \in S} d^2(\tilde{s}_1, \hat{s}_1) \tag{4.5}$$

$$\hat{s}_2 = \arg \min_{\hat{s}_2 \in S} d^2(\tilde{s}_2, \hat{s}_2) \tag{4.6}$$

where $\arg \min_{x \in S} d^2(\tilde{s}_i, \hat{s}_i)$ denotes the global minimum Euclidean distance between $\tilde{s}_i$ and $\hat{s}_i$

within the constellation set $S$ and $\hat{s}_i$ is the estimate of $s_i$ that was sent.

The above STF code can achieve a full diversity of four, with a transmit diversity
of two (two transmit antenna) and a frequency diversity of two (two receiving OFDM
subcarriers) assuming that all channel taps are uncorrelated. However, this comes at a
cost of twice the required bandwidth when compared to the standard Alamouti code since
it requires two subcarriers to achieve frequency diversity.

## C. CHANNEL TAP CORRELATION IN THE FREQUENCY DOMAIN

Consider a frequency-selective, quasi-static Rayleigh channel with $L$ resolvable multipaths. A MISO system with two transmit antennas and one receive antenna using OFDMA is used for signal transmission within this channel. The transmit antennas are assumed to have uncorrelated fading in the spatial domain. The OFDMA signal divides the broadband frequency-selective channel into $N$ parallel narrowband frequency-flat channels, each of which is modulated onto a single OFDMA subcarrier, and $N \gg L$. Two of the OFDMA subcarriers are chosen such that they each modulate a space-time code to form a space-time-frequency code for a single user; the code matrix is given in (4.1). Due to the fact that $N \gg L$, the two chosen subcarriers may be correlated to different degrees depending on their frequency separation and the coherence bandwidth of the channel.

Let the channel taps $h_{ij}$ be complex Gaussian-distributed random variables with unity variance such that $i \in \{1, 2\}$ denotes the subcarrier and $j \in \{1, 2\}$ denotes the transmit antenna. Denoting $\boldsymbol{h}_1 = [h_{11} \quad h_{12}]^T$, $\boldsymbol{h}_2 = [h_{21} \quad h_{22}]^T$ and $\boldsymbol{h} = [\boldsymbol{h}_1^T \quad \boldsymbol{h}_2^T]^T$, we define the correlation matrix between the channel taps as

$$R_{hh} = \mathrm{E}\{\boldsymbol{h}\boldsymbol{h}^T\} = \mathrm{E}\left\{ \begin{bmatrix} |h_{11}|^2 & h_{11}h_{12}^* & h_{11}h_{21}^* & h_{11}h_{22}^* \\ h_{12}h_{11}^* & |h_{12}|^2 & h_{12}h_{21}^* & h_{12}h_{22}^* \\ h_{21}h_{11}^* & h_{21}h_{12}^* & |h_{21}|^2 & h_{21}h_{22}^* \\ h_{22}h_{11}^* & h_{22}h_{12}^* & h_{22}h_{21}^* & |h_{22}|^2 \end{bmatrix} \right\}. \tag{4.7}$$

Given that the channel taps are spatially uncorrelated, the correlation factor $\mathrm{E}\{h_{ij}h_{i'j'}^*\}$ must be zero when $j \neq j'$. This assumption reduces (4.7) to

$$R_{hh} = \mathrm{E}\left\{ \begin{bmatrix} |h_{11}|^2 & 0 & h_{11}h_{21}^* & 0 \\ 0 & |h_{12}|^2 & 0 & h_{12}h_{22}^* \\ h_{21}h_{11}^* & 0 & |h_{21}|^2 & 0 \\ 0 & h_{22}h_{12}^* & 0 & |h_{22}|^2 \end{bmatrix} \right\}. \tag{4.8}$$

43

Equation (4.8) implies that the correlation matrix can be rewritten by considering the channel correlation matrix between the two antennas separately (since they have uncorrelated channel taps), such that

$$R_{h_1 h_1} = \mathrm{E} \left\{ \begin{bmatrix} |h_{11}|^2 & h_{11} h_{21}^* \\ h_{21} h_{11}^* & |h_{21}|^2 \end{bmatrix} \right\}$$
$$= \begin{bmatrix} 1 & r_1 \\ r_1 & 1 \end{bmatrix} \qquad (4.9)$$

$$R_{h_2 h_2} = \mathrm{E} \left\{ \begin{bmatrix} |h_{12}|^2 & h_{12} h_{22}^* \\ h_{22} h_{12}^* & |h_{22}|^2 \end{bmatrix} \right\}$$
$$= \begin{bmatrix} 1 & r_2 \\ r_2 & 1 \end{bmatrix} \qquad (4.10)$$

where $r_i$ is a correlation factor. Furthermore, since the channel statistics are the same for all $h_{ij}$, i.e., the means and variances of all $h_{ij}$ are 0 and 1, respectively, it follows that $r_1 = r_2$. This implies that the correlation factor is simply a function of the frequency separation between the two subcarriers and the coherence bandwidth of the channel. This correlation factor between the channel taps in the frequency domain is denoted as $r$. Therefore, when $r = 0$, the channel taps are completely uncorrelated, resulting from a frequency-selective channel with sufficient resolvable paths $L \geq 2$ and two properly chosen OFDM subcarrier frequencies much greater than the coherence bandwidth. In this case, the maximum achievable diversity order is four. When $r = 1$, the channel is either frequency-flat ($L = 1$) or the two subcarriers are so closely spaced that they exhibit complete correlation. In this case, the maximum diversity order is only two (which comes from the spatial domain).

# VI.   PERFORMANCE EVALUATION AND ANALYSIS FOR SPACE-TIME-FREQUENCY CODES

In this chapter, we evaluate the achievable diversity gains in both the space and frequency domains using the space-time-frequency (STF) block code that was designed in Section V.B, as well as compare performance with the space-time block codes (STBC) designed in Chapter III.

## A.   SPACE-FREQUENCY DIVERSITY PERFORMANCE OF STF CODES

Consider the frequency-selective, quasi-static Rayleigh channel described in Section V.C. A MISO system with two transmit antennas and one receive antenna using two OFDM subcarriers is used for signal transmission within this channel. A space-time-frequency (STF) code given in (4.1) is used to modulate the signal across both subcarriers. The bit error rate (BER) performance of the system is evaluated with varying correlation between the two subcarrier frequencies, representing the frequency diversity available under different frequency-selectivity conditions of the channel, i.e., the power-delay profile of the channel. The baseband modulations used are QPSK, 16-QAM and 64-QAM. The chosen correlation factors between the two frequencies are 1.0 (frequency-flat channel), 0.9, 0.5, and 0 (frequency-selective channel with independent fading in the frequency domain).

The results of the simulation for QPSK, 16-QAM, and 64-QAM modulation are shown in Figures 14 through 16, respectively. The notation "2:1" in the legend is interpreted as two transmit antenna and one OFDM subcarrier (i.e., standard Alamouti with two transmit and one receive antenna), while "2:2" is interpreted as two transmit antenna and two OFDM subcarriers (equivalent to two transmit and two receive antenna from the perspective of total achievable diversity).
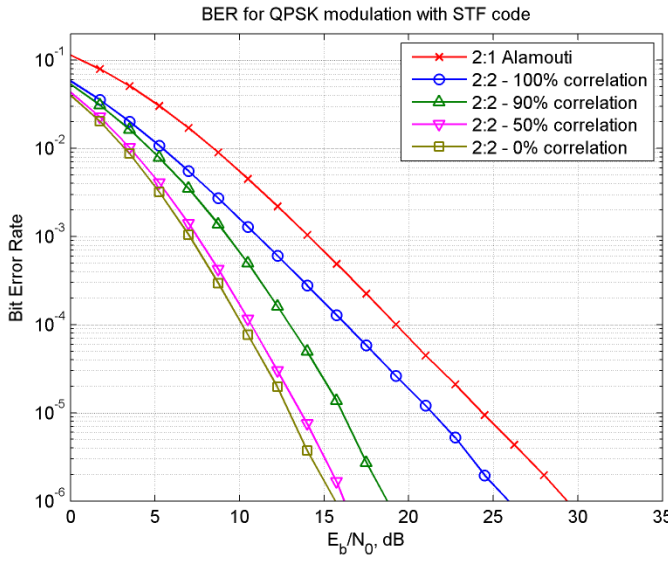
Figure 14.        BER for STF code using QPSK.
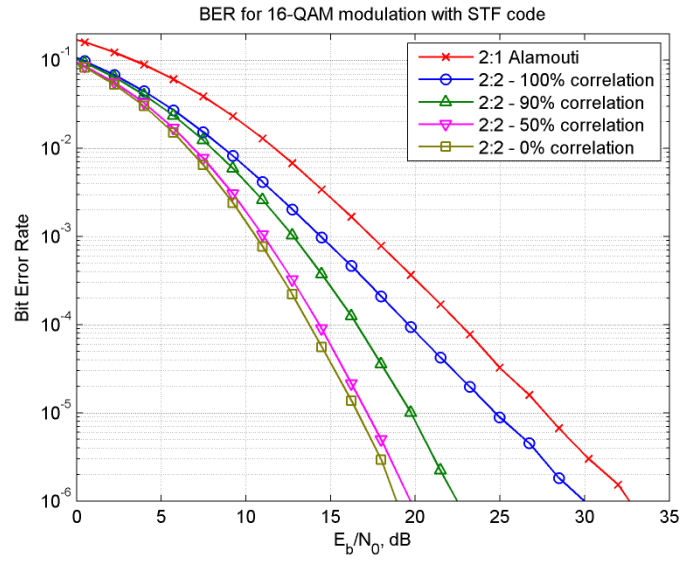


Figure 15.        BER for STF code using 16-QAM.
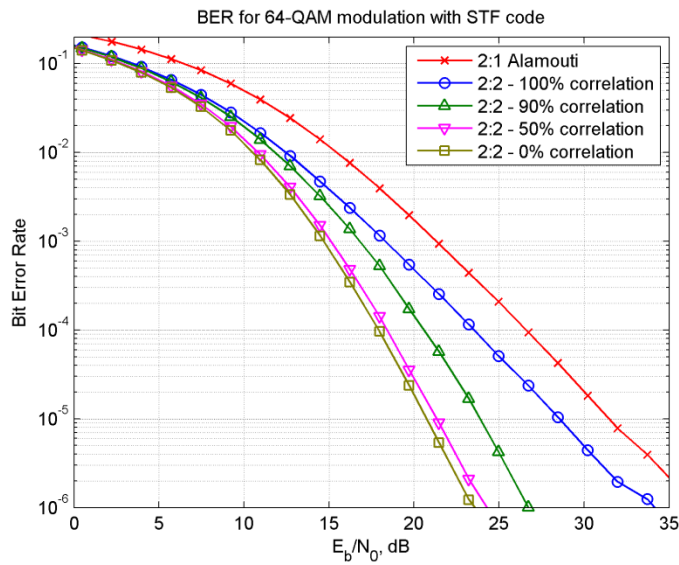


Figure 16.        BER for STF code using 64-QAM.

It can be seen that for all three modulation schemes, the BER performance has the same characteristics except for horizontal shifts in the BER with respect to $E_b/N_0$. This lends itself to a discussion of the characteristics of the results in general without any specifics relating to any particular modulation scheme used.

46

Firstly, the performance of the 2:2 scheme with 100% correlation achieves only a diversity of two, as it has the same gradient as the 2:1 Alamouti scheme in the higher $E_b/N_0$ region. This is because in a frequency-flat channel, there is no frequency-diversity available to exploit, therefore, the only diversity is in the spatial domain from the two transmit antennas. However, there is a 3 dB gain in BER performance across the entire $E_b/N_0$ range when comparing the 2:2 with 100% correlation to the 2:1 Alamouti. This gain in performance comes from having two separate OFDM subcarriers that are sending the same signal, resulting in a received signal with twice the power of one subcarrier. However, this requires twice the bandwidth of one subcarrier as well, i.e., the 2:2 STF code only has half the bandwidth efficiency of the 2:1 Alamouti STBC.

The 2:2 scheme with 0% correlation achieves a full diversity of order four, as the gradient in the higher $E_b/N_0$ region is approximately twice that of the diversity two performance. This is a result of achieving a diversity order of two from both the spatial and frequency domain. A frequency-selective channel, which would present a challenging inter-symbol interference problem for a broadband single carrier modulation, has turned out to be extremely beneficial for a frequency-diversity scheme utilizing multiple subcarriers such as OFDM.

The BER performance when there is partial correlation between the two channel taps in the frequency domain with correlation factors of 0.5 and 0.9 are also shown in Figure 14 through Figure 16. The frequency diversity performance of those simulations is somewhere between that of perfect correlation ($r = 1$) and no correlation ($r = 0$). Interestingly, even when the channel taps exhibit a strong correlation at 0.9, the BER performance is still significantly better than a frequency-flat channel, especially in the higher $E_b/N_0$ region. For example, at a BER of $10^{-6}$, the $r = 0.9$ curves have a diversity gain of approximately 7 to 8 dB when compared to the $r = 1$ curves for all modulation schemes. For the $r = 0.5$ curves, the BER performance closely tracks that of the perfectly uncorrelated channel taps ($r = 0$), with less than 1 dB difference at a BER of $10^{-6}$. This implies that given a frequency-selective channel, the STF code in (4.1) allows the extraction of a significant amount of frequency diversity, even when the channels taps are

somewhat correlated, especially if the correlation is less than 0.5. This supports the definition of the coherence bandwidth given in (2.1), which is based on 50% correlation ([2]). When $r \leq 0.5$, the BER performance is almost on par with uncorrelated channel taps ($r = 0$), with less than 1 dB difference at a BER of $10^{-6}$.

## B.  ANALYSIS OF FREQUENCY RESPONSE CORRELATIONS

To gain a better understanding of the meaning of the correlated frequency responses presented in the previous section, simulations were performed to study the relationship between the power-delay profile of a fading channel and its coherence bandwidth as well as the correlation with respect to the frequency separation between two frequencies. The simulation used the six-ray Typical Urban (TU) model from COST 207 ([20]). The model parameters are as given in Table 5.

Table 5.      COST 207 six-ray typical urban model parameters.

| Delay (µs) | 0 | 0.2 | 0.5 | 1.6 | 2.3 | 5.0 |
|---|---|---|---|---|---|---|
| Fractional Power | 0.189 | 0.379 | 0.239 | 0.095 | 0.061 | 0.037 |

Using the parameters, we calculate the mean delay $\bar{\tau}$ and delay spread $\sigma_\tau$ as

$$\bar{\tau} = \frac{\sum_l p_l \tau_l}{\sum_l p_l} = \frac{0.189 \times 0 + 0.379 \times 0.2 + 0.239 \times 0.5 + 0.095 \times 1.6 + 0.061 \times 2.3 + 0.037 \times 5.0}{0.189 + 0.379 + 0.239 + 0.095 + 0.061 + 0.037} = 0.673 \ \mu s$$

$$\overline{\tau^2} = \frac{\sum_l p_l \tau_l}{\sum_l p_l} = \frac{0.189 \times 0^2 + 0.379 \times 0.2^2 + 0.239 \times 0.5^2 + 0.095 \times 1.6^2 + 0.061 \times 2.3^2 + 0.037 \times 5.0^2}{0.189 + 0.379 + 0.239 + 0.095 + 0.061 + 0.037} = 1.566 \ \mu s^2$$

$$\sigma_\tau = \sqrt{\overline{\tau^2} - (\bar{\tau})^2} = 1.06 \ \mu s.$$

The 50% coherence bandwidth is thus given as

$$B_c = \frac{1}{5\sigma_\tau} \approx 190 \text{ kHz}. \tag{4.11}$$

The first step was to generate 100,000 realizations of the model and extract all of the six channel taps in every realization. The frequency response $H(f)$ was then calculated for every realization across a range of 1 MHz. Since the channel is assumed

static, it is assumed that the frequency response is wide sense stationary and the correlation in the frequency response solely depends upon the frequency difference $\Delta f$ and not on the absolute frequency. The correlation in the channel gain $|H(f)|$ with respect to $\Delta f$ is calculated and shown in Figure 17.
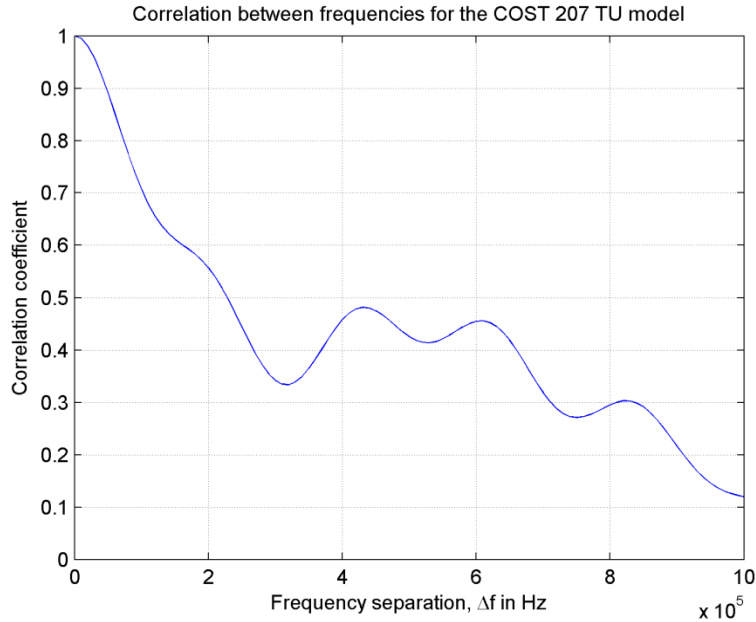


Figure 17.    Correlation of channel gain with respect to $\Delta f$.

It can be deduced by inspection of Figure 17 that the 50% correlation bandwidth is approximately 230 kHz, which is close to the calculated coherence bandwidth of 190 kHz as shown in (4.11). Also, the 90% correlation bandwidth is around 50 kHz. Therefore, for the COST 207 TU model, a modulator using two subcarriers at least 230 kHz apart should have a performance similar to as the one predicted by the 50% correlation curves presented in Figure 14 through Figure 16 in the previous section. Choosing subcarriers that are spaced at least 50 kHz apart should lead to a performance similar to as the one predicted by the 90% correlation curves. In addition, it may be of interest to note that in Figure 17, even with subcarriers of 1 MHz spacing, the correlation is around 0.1, implying that the channel taps are still not completely independent.

Therefore, complete independence of the channel taps in the frequency domain may not be easily achieved without having a large allocated bandwidth.

## C. COMPARISON OF SPATIAL DIVERSITY AND SPACE-FREQUENCY DIVERSITY

Thus far, this thesis has discussed two methods of obtaining a diversity order of four, harnessing a spatial diversity order of four using four transmit antennas and harnessing space-frequency diversity of order two in each domain using two transmit antennas and two separate uncorrelated frequencies. In this section, a comparison of the performance of the space-time codes and space-time-frequency codes that have a full diversity of order four is presented. Specifically, the half-rate orthogonal space-time block codes (denoted as O-STBC 8×4) is compared[2] to the full rate space-time-frequency codes with uncorrelated taps in the frequency domain (denoted as STFC 2:2). The diversity four codes used for comparison are listed in Table 6.

Table 6.    List of codes with a diversity order of four used for comparison.

| Modulation | Code type | Code rate | Normalized bandwidth | Normalized bandwidth efficiency |
|---|---|---|---|---|
| QPSK | O-STBC 8×4 | 0.5 | 1 Hz | 1 bps/Hz |
| QPSK | STFC 2:2 | 1 | 2 Hz | 1 bps/Hz |
| 16-QAM | O-STBC 8×4 | 0.5 | 1 Hz | 2 bps/Hz |
| 16-QAM | STFC 2:2 | 1 | 2 Hz | 2 bps/Hz |
| 64-QAM | O-STBC 8×4 | 0.5 | 1 Hz | 3 bps/Hz |
| 64-QAM | STFC 2:2 | 1 | 2 Hz | 3 bps/Hz |

The plot of the comparison in BER performance between STBC and STFC in the various modulation schemes (QPSK, 16-QAM and 64-QAM) is shown in Figure 18.

---

[2] The comparison for QO-STBC with the O-STBC has already been made in Sections IV.B.2 and IV.B.3. In summary, the QO-STBC and O-STBC had very comparable performance when the bandwidth efficiency is the same. The reader is encouraged to cross-reference to those sections for the details to understand the relative performance between STFC and QO-STBC.
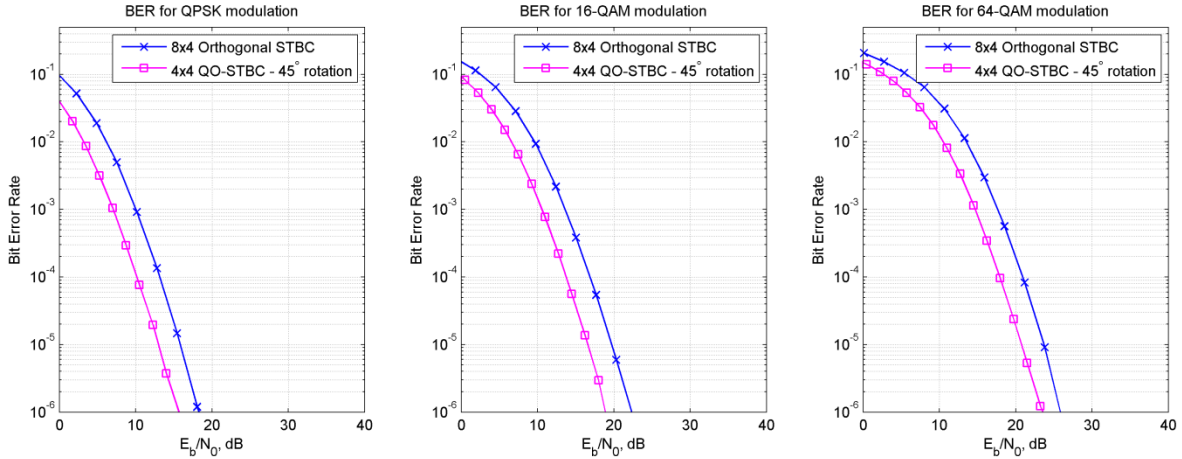
Figure 18.    BER comparison between STBC and STFC with a diversity order of four.

The STFC outperforms the O-STBC by 3 dB across the entire $E_b / N_0$ range. This is because the power at the transmit antennas for the STFC is split across two antennas, while the power is split across four antennas for the O-STBC. This results in twice the amount of transmit power for the STFC compared to the O-STBC, which gives a 3 dB gain. Also, note that the bandwidth efficiency of the STFC and the O-STBC are the same. The STFC has unity-rate but requires a normalized bandwidth of 2 Hz, while the O-STBC has half-rate, but uses a normalized bandwidth of 1 Hz. Therefore, the STFC has distinct advantages over the O-STBC in that it requires only two antennas (savings in hardware cost and implementation complexity) and has a gain of 3 dB compared to the O-STBC. However, this is only feasible if the coherence bandwidth is sufficiently small for frequency diversity to be exploited. Furthermore, in a Doppler channel where the fading is time-variant, there will be design constraints on the number of OFDM subcarriers that can be chosen. On one hand, the number of subcarriers $N$ must be sufficiently large to ensure that each subcarrier bandwidth is within the coherence bandwidth of the channel, but $N$ must also be sufficiently small to ensure that the OFDM symbol time is within the coherence time. These constraints may result in the inability to achieve full frequency diversity (the effects of which were analyzed in Section VI.A) and, thus, lose the advantages of the STFC.

## D. CONCLUSION

STF codes are able to combat fade effectively by harnessing frequency diversity on top of the spatial diversity. In addition, the channel taps do not need to be completely uncorrelated to achieve good performance. A good rule of thumb is that any correlation of less than 0.5 will perform almost as well as the best achievable performance of independent channel taps.

Also, STF codes provide a 3 dB advantage over STBC with comparable bandwidth efficiency. This makes STF code particular attractive since it saves the cost of additional antennas but requires the use of OFDM, which increases the complexity of modulation/demodulation. Also, the channel has to be frequency-selective in order for STF codes to be effective, and the effects of a Doppler channel may be detrimental to the implementation of STF codes due to the design constraints of choosing the number of OFDM subcarriers.

# VII. CONCLUSION

In this thesis, we examined how to exploit diversity in both the spatial and frequency domains depending on the channel conditions available. We have also explored the level of diversity available in both the space and frequency domains, and how performance is affected by the code design (constellation rotation for the space domain) and varying channel conditions (frequency-selectivity of the channel affecting the correlation of the channel taps).

## A. SIGNIFICANT FINDINGS

To harness spatial diversity, a MIMO system with multiple antennas is required. Furthermore, the channel taps from each pair of transmit-receive antennas have to be uncorrelated for spatial diversity to be present. The number of antennas present limits the maximum available diversity, as evidenced by the exploration of systems with either two or four transmit antennas with a single receiving antenna. In addition, when more than two antennas are used, full diversity is only possible with either a non-unity rate orthogonal code or a unity-rate quasi-orthogonal (QO) code. In the case of quasi-orthogonal codes, full diversity is only achievable through constellation rotation.

Simulation was used to show that, while the diversity product used for determining the angle of rotation to achieve full diversity is a sufficient statistics, it is not a necessary one, as illustrated by the simulation of the 64-QAM QO space-time block codes (STBC) with three different angles with different diversity products that achieved full diversity.

In addition, the QO-STBC with constellation rotation is a viable and preferred method to achieve a diversity order of four when compared to the orthogonal half-rate STBC, as its performance is better with higher order modulations. It is also possible that QO-STBC will have less performance degradation in a Doppler channel compared to orthogonal STBC due to the fact that the block time of a QO-STBC is only half that of the orthogonal STBC (four time slots compared to eight respectively). A shorter

time block will have channels taps with higher correlations in the time domain and, hence, more accurate channel tap estimates. However, this was not explicitly simulated or proven.

The examination of space-frequency diversity introduced the concept of duplicating the signal in the frequency domain to improve the reliability of transmission. However, a frequency-selective channel is necessary to exploit this diversity. Through simulation, we illustrated the varying degrees of performance degradation in the event of channel correlations in the frequency domain, and established an example of what channel correlations are like using the COST 207 six-ray Typical Urban model. Even with channel correlations of up to 0.5, the performance of the space-time-frequency code still closely matches that of independent channel taps. This supports the definition of coherence bandwidth, which is also based on 50% correlation.

## B.    RECOMMENDATION FOR FUTURE WORK

Inspired by the findings in this thesis, there are many possibilities for follow-up work that can further explore the concept of maximizing the performance of a communications system in a fading channel. Some of the suggestions are as follows.

### 1.    System Performance With Channel Feedback

We have assumed that the transmitter has no knowledge of the channel conditions, while the receiver has perfect channel state information. One could study the performance improvements that are possible if the receiver can channel feedback to the transmitter so that the transmitter can more appropriately allocate its power to the different transmit antennas.

### 2.    System Degradation With Spatial Correlations

We also assumed perfect spatial decorrelation. Studies can be performed to determine the amount of degradation if the channel taps are correlated in the spatial domains. Antenna topology and geometry would have to be explored to determine their impact on spatial correlations.

### 3. Impact of Doppler Channels and Time Diversity

Another assumption made in this thesis was that of a quasi-static channel. However, a fading channel is likely to be time-varying, especially for portable communication systems, which creates the opportunity to exploit time diversity. However, exploiting time diversity is challenging because if the channel changes too slowly, then time-sensitive applications (e.g., telephony) will not be feasible. However, if the channel changes too quickly, the channel becomes time-selective and accurate estimates of channel taps become difficult. Studies into schemes that can correct for Doppler and exploit time-diversity would allow a code to achieve diversity in all three diversity domains of space, time and frequency.

THIS PAGE INTENTIONALLY LEFT BLANK

# APPENDIX A – DERIVATION OF CHANNEL TAP MATRIX

The derivation for the channel tap matrix, $H$, for both the rate ½ orthogonal code and the rate 1 quasi-orthogonal codes given in sections III.B.2 and III.C.1, respectively, are given in this appendix.

## A.	RATE ½ ORTHOGONAL 4X DIVERSITY CODE

The code matrix of the rate ½ orthogonal code is given by

$$G = \begin{bmatrix} s_1 & s_2 & s_3 & s_4 \\ -s_2 & s_1 & -s_4 & s_3 \\ -s_3 & s_4 & s_1 & -s_2 \\ -s_4 & -s_3 & s_2 & s_1 \\ s_1^* & s_2^* & s_3^* & s_4^* \\ -s_2^* & s_1^* & -s_4^* & s_3^* \\ -s_3^* & s_4^* & s_1^* & -s_2^* \\ -s_4^* & -s_3^* & s_2^* & s_1^* \end{bmatrix}. \tag{1.1}$$

Denoting $h_i = |h_i| e^{j\theta_i}, i = 1, 2, 3, 4$ where $h_i$ is the channel tap corresponding to transmit antenna $i$ to the receiving antenna, we have

$$r = \sqrt{\frac{\rho}{n}} Gh + n$$

$$
\begin{bmatrix} r_1 \\ r_2 \\ r_3 \\ r_4 \\ r_5 \\ r_6 \\ r_7 \\ r_8 \end{bmatrix}
= \sqrt{\frac{\rho}{4}}
\begin{bmatrix}
s_1 & s_2 & s_3 & s_4 \\
-s_2 & s_1 & -s_4 & s_3 \\
-s_3 & s_4 & s_1 & -s_2 \\
-s_4 & -s_3 & s_2 & s_1 \\
s_1^* & s_2^* & s_3^* & s_4^* \\
-s_2^* & s_1^* & -s_4^* & s_3^* \\
-s_3^* & s_4^* & s_1^* & -s_2^* \\
-s_4^* & -s_3^* & s_2^* & s_1^*
\end{bmatrix}
\begin{bmatrix} h_1 \\ h_2 \\ h_3 \\ h_4 \end{bmatrix}
+
\begin{bmatrix} n_1 \\ n_2 \\ n_3 \\ n_4 \\ n_5 \\ n_6 \\ n_7 \\ n_8 \end{bmatrix}
$$

$$
= \sqrt{\frac{\rho}{4}}
\begin{bmatrix}
h_1 s_1 + h_2 s_2 + h_3 s_3 + h_4 s_4 \\
h_2 s_1 - h_1 s_2 - h_3 s_4 + h_4 s_3 \\
h_3 s_1 - h_1 s_3 + h_2 s_4 - h_4 s_2 \\
h_3 s_2 - h_2 s_3 - h_1 s_4 + h_4 s_1 \\
s_1 h_1^* + s_2 h_2^* + s_3 h_3^* + s_4 h_4^* \\
s_1 h_2^* - s_2 h_1^* + s_3 h_4^* - s_4 h_3^* \\
s_1 h_3^* - s_3 h_1^* - s_2 h_4^* + s_4 h_2^* \\
s_1 h_4^* + s_2 h_3^* - s_3 h_2^* - s_4 h_1^*
\end{bmatrix}
+
\begin{bmatrix} n_1 \\ n_2 \\ n_3 \\ n_4 \\ n_5 \\ n_6 \\ n_7 \\ n_8 \end{bmatrix}
\qquad (1.2)
$$

where $r_i$ denotes the received vector at time slot $i$, $\rho$ denotes the signal-to-noise ratio, and $n_i$ denotes the normalized noise vector with variance 2 at time $i$. The factor of $n = 4$ in $\sqrt{\frac{\rho}{n}}$ represents the normalizing of the transmitter power across four antenna.

Remapping the received vector by taking the complex conjugate of $r_5$ to $r_8$ and denoting it as vector $Y$, we can express the system model as

$$
\begin{bmatrix} r_1 \\ r_2 \\ r_3 \\ r_4 \\ r_5^* \\ r_6^* \\ r_7^* \\ r_8^* \end{bmatrix} = \sqrt{\frac{\rho}{4}} \begin{bmatrix} h_1 s_1 + h_2 s_2 + h_3 s_3 + h_4 s_4 \\ h_2 s_1 - h_1 s_2 + h_4 s_3 - h_3 s_4 \\ h_3 s_1 - h_4 s_2 - h_1 s_3 + h_2 s_4 \\ h_4 s_1 + h_3 s_2 - h_2 s_3 - h_1 s_4 \\ h_1^* s_1 + h_2^* s_2 + h_3^* s_3 + h_4^* s_4 \\ h_2^* s_1 - h_1^* s_2 + h_4^* s_3 - h_3^* s_4 \\ h_3^* s_1 - h_4^* s_2 - h_1^* s_3 + h_2^* s_4 \\ h_4^* s_1 + h_3^* s_2 - h_2^* s_3 - h_1^* s_4 \end{bmatrix} + \begin{bmatrix} n_1 \\ n_2 \\ n_3 \\ n_4 \\ n_5^* \\ n_6^* \\ n_7^* \\ n_8^* \end{bmatrix}
$$

$$
Y = \sqrt{\frac{\rho}{4}} \begin{bmatrix} h_1 & h_2 & h_3 & h_4 \\ h_2 & -h_1 & h_4 & -h_3 \\ h_3 & -h_4 & -h_1 & h_2 \\ h_4 & h_3 & -h_2 & -h_1 \\ h_1^* & h_2^* & h_3^* & h_4^* \\ h_2^* & -h_1^* & h_4^* & -h_3^* \\ h_3^* & -h_4^* & -h_1^* & h_2^* \\ h_4^* & h_3^* & -h_2^* & -h_1^* \end{bmatrix} \begin{bmatrix} s_1 \\ s_2 \\ s_3 \\ s_4 \end{bmatrix} + \begin{bmatrix} n_1 \\ n_2 \\ n_3 \\ n_4 \\ n_5^* \\ n_6^* \\ n_7^* \\ n_8^* \end{bmatrix} \tag{1.3}
$$

$$
Y = \sqrt{\frac{\rho}{4}} Hs + N
$$

where the channel tap matrix $H$ is given by

$$
H = \begin{bmatrix} h_1 & h_2 & h_3 & h_4 \\ h_2 & -h_1 & h_4 & -h_3 \\ h_3 & -h_4 & -h_1 & h_2 \\ h_4 & h_3 & -h_2 & -h_1 \\ h_1^* & h_2^* & h_3^* & h_4^* \\ h_2^* & -h_1^* & h_4^* & -h_3^* \\ h_3^* & -h_4^* & -h_1^* & h_2^* \\ h_4^* & h_3^* & -h_2^* & -h_1^* \end{bmatrix}. \tag{1.4}
$$

## B. RATE 1 QUASI-ORTHOGONAL (QO) 4X DIVERSITY CODE

The code matrix of the rate 1 QO-STBC is given by

$$
G = \begin{bmatrix} s_1 & s_2 & s_3 & s_4 \\ s_2^* & -s_1^* & s_4^* & -s_3^* \\ s_3 & -s_4 & -s_1 & s_2 \\ s_4^* & s_3^* & -s_2^* & -s_1^* \end{bmatrix}. \tag{1.5}
$$

Denoting $h_i = |h_i| e^{j\theta_i}$, $i = 1, 2, 3, 4$ where $h_i$ is the channel tap corresponding to transmit antenna $i$ to the receiving antenna, we have

$$r = \sqrt{\frac{\rho}{n}} Gh + n$$

$$\begin{bmatrix} r_1 \\ r_2 \\ r_3 \\ r_4 \end{bmatrix} = \sqrt{\frac{\rho}{4}} \begin{bmatrix} s_1 & s_2 & s_3 & s_4 \\ s_2^* & -s_1^* & s_4^* & -s_3^* \\ s_3 & -s_4 & -s_1 & s_2 \\ s_4^* & s_3^* & -s_2^* & -s_1^* \end{bmatrix} \begin{bmatrix} h_1 \\ h_2 \\ h_3 \\ h_4 \end{bmatrix} + \begin{bmatrix} n_1 \\ n_2 \\ n_3 \\ n_4 \end{bmatrix} \qquad (1.6)$$

$$= \sqrt{\frac{\rho}{4}} \begin{bmatrix} h_1 s_1 + h_2 s_2 + h_3 s_3 + h_4 s_4 \\ h_1 s_2^* - h_2 s_1^* + h_3 s_4^* - h_4 s_3^* \\ h_1 s_3 - h_3 s_1 - h_2 s_4 + h_4 s_2 \\ h_1 s_4^* + h_2 s_3^* - h_3 s_2^* - h_4 s_1^* \end{bmatrix} + \begin{bmatrix} n_1 \\ n_2 \\ n_3 \\ n_4 \end{bmatrix}$$

where $r_i$ denotes the received vector at time slot $i$, $\rho$ denotes the signal-to-noise ratio, and $n_i$ denotes the normalized noise vector with variance 2 at time $i$. The factor of $n = 4$ in $\sqrt{\frac{\rho}{n}}$ represents the normalizing of the transmitter power across four antenna.

Remapping the received vector by taking the complex conjugate of $r_2$ to $r_4$ and denoting it as vector $Y$, we can express the system model as

$$\begin{bmatrix} r_1 \\ r_2^* \\ r_3 \\ r_4^* \end{bmatrix} = \sqrt{\frac{\rho}{4}} \begin{bmatrix} h_1 s_1 + h_2 s_2 + h_3 s_3 + h_4 s_4 \\ -h_2^* s_1 + h_1^* s_2 - h_4^* s_3 + h_3^* s_4 \\ -h_3 s_1 + h_4 s_2 + h_1 s_3 - h_2 s_4 \\ -h_4^* s_1 - h_3^* s_2 + h_2^* s_3 + h_1^* s_4 \end{bmatrix} + \begin{bmatrix} n_1 \\ n_2^* \\ n_3 \\ n_4^* \end{bmatrix}$$

$$Y = \sqrt{\frac{\rho}{4}} \begin{bmatrix} h_1 & h_2 & h_3 & h_4 \\ -h_2^* & h_1^* & -h_4^* & h_3^* \\ -h_3 & h_4 & h_1 & -h_2 \\ -h_4^* & -h_3^* & h_2^* & h_1^* \end{bmatrix} \begin{bmatrix} s_1 \\ s_2 \\ s_3 \\ s_4 \end{bmatrix} + \begin{bmatrix} n_1 \\ n_2^* \\ n_3 \\ n_4^* \end{bmatrix} \qquad (1.7)$$

$$Y = \sqrt{\frac{\rho}{4}} Hs + N$$

where the channel tap matrix $H$ is given by

$$\boldsymbol{H} = \begin{bmatrix} h_1 & h_2 & h_3 & h_4 \\ -h_2^* & h_1^* & -h_4^* & h_3^* \\ -h_3 & h_4 & h_1 & -h_2 \\ -h_4^* & -h_3^* & h_2^* & h_1^* \end{bmatrix}. \tag{1.8}$$

THIS PAGE INTENTIONALLY LEFT BLANK

# APPENDIX B – SOURCE CODE

**ML_O-STBC.m**

This file is used to do the simulation of the O-STBC with maximum likelihood decoding.

```matlab
clear
close all
% clc
load constellation_map

N = logspace (log10(1e6),log10(9e8), 20); % number of bits or symbols
EbN0_lower = 0;
EbN0_upper = 50;
num_EbN0_points = 20;
num_points_per_iter = 6e4;

for modulation_type = 2:4

switch modulation_type
    case {1,2}
        m=modulation_type;
    case 3
        m=4;
    case 4
        m=6;
end

num_iter = ceil(N/num_points_per_iter/m);


disp (sprintf('Simulating modulation type: %d', modulation_type));

% modulation_type=1;
% m=2;
% select modulation scheme
switch m
    case 1
        constellation_map = bpsk_map;
        c_factor = 1;
    case 2
        constellation_map = qpsk_map;
        c_factor = sqrt(2);
    case 4
        constellation_map = qam16_map;
        c_factor = sqrt(10);
    case 6
        constellation_map = qam64_map;
        c_factor = sqrt(42);
end


% initialise variables
Eb_N0_dB = linspace(EbN0_lower,EbN0_upper,num_EbN0_points) ; % multiple Eb/N0 values
num_bit_errors_2xdiversity = zeros(1, num_EbN0_points);
num_bit_errors_4xdiversity_ortho = zeros(1, num_EbN0_points);

tic
for j_iter = 1:num_EbN0_points
    for i_iter = 1:num_iter(j_iter)
        % Transmitter
        symbol_orig = randi([0 2^m-1],num_points_per_iter,1) ;
        s = constellation_map(symbol_orig+1);

        % white gaussian noise, 0dB variance
        n1 = 1/sqrt(2)*(randn(num_points_per_iter,1) + 1i*randn(num_points_per_iter,1));
        n2 = 1/sqrt(2)*(randn(num_points_per_iter,1) + 1i*randn(num_points_per_iter,1));
        n3 = 1/sqrt(2)*(randn(num_points_per_iter,1) + 1i*randn(num_points_per_iter,1));
        n4 = 1/sqrt(2)*(randn(num_points_per_iter,1) + 1i*randn(num_points_per_iter,1));
        n5 = 1/sqrt(2)*(randn(num_points_per_iter,1) + 1i*randn(num_points_per_iter,1));
        n6 = 1/sqrt(2)*(randn(num_points_per_iter,1) + 1i*randn(num_points_per_iter,1));
        n7 = 1/sqrt(2)*(randn(num_points_per_iter,1) + 1i*randn(num_points_per_iter,1));
        n8 = 1/sqrt(2)*(randn(num_points_per_iter,1) + 1i*randn(num_points_per_iter,1));

        h1 = 1/sqrt(2)*(randn(num_points_per_iter,1) + 1i*randn(num_points_per_iter,1)); % Rayleigh channel
        h2 = 1/sqrt(2)*(randn(num_points_per_iter,1) + 1i*randn(num_points_per_iter,1)); % Rayleigh channel
        h3 = 1/sqrt(2)*(randn(num_points_per_iter,1) + 1i*randn(num_points_per_iter,1)); % Rayleigh channel
        h4 = 1/sqrt(2)*(randn(num_points_per_iter,1) + 1i*randn(num_points_per_iter,1)); % Rayleigh channel
        h5 = 1/sqrt(2)*(randn(num_points_per_iter,1) + 1i*randn(num_points_per_iter,1)); % Rayleigh channel
        h6 = 1/sqrt(2)*(randn(num_points_per_iter,1) + 1i*randn(num_points_per_iter,1)); % Rayleigh channel
        h7 = 1/sqrt(2)*(randn(num_points_per_iter,1) + 1i*randn(num_points_per_iter,1)); % Rayleigh channel
        h8 = 1/sqrt(2)*(randn(num_points_per_iter,1) + 1i*randn(num_points_per_iter,1)); % Rayleigh channel

        % Channel and noise Noise addition
```

```matlab
            div2noise_factor = sqrt(2)*(10^(-Eb_N0_dB(j_iter)/20));
            div4noise_factor = 2*sqrt(2)*(10^(-Eb_N0_dB(j_iter)/20));

            y_2xdiversity = s                    - div2noise_factor .*              (conj(h1).*n1   +  h2.*n2) ./
(h1.*conj(h1) + h2.*conj(h2));
            y_4xdiversity_ortho = s - div4noise_factor * (   h1.*n5 + h2.*n6 + h3.*n7 + h4.*n8 + n1.*conj(h1) +
n2.*conj(h2) + n3.*conj(h3) + n4.*conj(h4)   )   ./ (2*(h1.*conj(h1) + h2.*conj(h2) + h3.*conj(h3) + h4.*conj(h4))) ;

            % receiver - hard decision symbol decoding
            [dummy, sort_index] = sort (abs(constellation_map*ones(1,num_points_per_iter) - ones(2^m,1)*y_2xdiversity.'));
            symbol_2xdiversity = sort_index(1,:).'-1;
            [dummy, sort_index] = sort (abs(constellation_map*ones(1,num_points_per_iter) -
ones(2^m,1)*y_4xdiversity_ortho.'));
            symbol_4xdiversity_ortho = sort_index(1,:).'-1;

            % count bit errors
            dummy = (s-constellation_map(symbol_2xdiversity+1)) * c_factor/2;
            num_bit_errors_2xdiversity(j_iter) = num_bit_errors_2xdiversity(j_iter) +
sum(bit_diff_map(round(abs(real(dummy)))+1)) + sum(bit_diff_map(round(abs(imag(dummy)))+1));
            dummy = (s-constellation_map(symbol_4xdiversity_ortho+1)) * c_factor/2;
            num_bit_errors_4xdiversity_ortho(j_iter) = num_bit_errors_4xdiversity_ortho(j_iter) +
sum(bit_diff_map(round(abs(real(dummy)))+1)) + sum(bit_diff_map(round(abs(imag(dummy)))+1));



            if mod (i_iter, 10)==1
                if j_iter>1
                    secsLeft = toc/(i_iter+sum(num_iter(1:j_iter-1)))  *   (num_iter(j_iter)-i_iter +
sum(num_iter(j_iter+1:num_EbN0_points)))   ;
                else
                    secsLeft = toc/(i_iter)*(num_iter(j_iter)-i_iter + sum(num_iter(j_iter+1:num_EbN0_points)))   ;
                end
                disp(sprintf('Estimated time remaining: %f seconds, ETA: %s', secsLeft, datestr(now+secsLeft/86400)        )
)
            end
        end
    end
end
N = num_iter * num_points_per_iter;

simBer_2xdiversity(modulation_type,:) = num_bit_errors_2xdiversity./N/m; % simulated ber
simBer_4xdiversity_ortho(modulation_type,:) = num_bit_errors_4xdiversity_ortho./N/m; % simulated ber

end

filename = ['myrun_ortho_new_' num2str(now) '.mat'];
save (filename)

EbN0_dB_QPSK = Eb_N0_dB - 10*log10(2);
EbN0_dB_QAM16 = Eb_N0_dB - 10*log10(4);
EbN0_dB_QAM64 = Eb_N0_dB - 10*log10(6);

EbN0_dB = [Eb_N0_dB; EbN0_dB_QPSK; EbN0_dB_QAM16; EbN0_dB_QAM64];

% plot
close all
figure
for i=2:4
    semilogy(EbN0_dB(i,:),simBer_2xdiversity(i,:),'rx-','LineWidth',1);
    hold on
end
for i=2:4
    semilogy(EbN0_dB(i,:),simBer_4xdiversity_ortho(i,:),'rx-','LineWidth',1);
    hold on
end

axis([EbN0_lower 40 10^-6 0.5])
grid on
legend('AWGN-Theory','Rayleigh-Simulation', 'Diversity-Simulation');
xlabel('Eb/No, dB');
ylabel('Bit Error Rate');
title('BER for BPSK modulation in Rayleigh channel');


% calculate theoretical QAM curves
M=16;
L=4;
iSNR = 3*10.^(Eb_N0_dB(1,:)/10)/L/2/(M-1);
mu = sqrt(iSNR./(1+iSNR));
sumterm = 0;
for l=0:L-1
    sumterm = sumterm + nchoosek(L-1+l, l)*((1+mu)/2).^l;
end
qam16BerTheory = (4-4/sqrt(M))/log2(M)*((1-mu)/2).^L .* sumterm;
semilogy (EbN0_dB_QAM16, qam16BerTheory, 'g')

M=64;
L=4;
iSNR = 3*10.^(Eb_N0_dB(1,:)/10)/L/2/(M-1);
mu = sqrt(iSNR./(1+iSNR));
sumterm = 0;
for l=0:L-1
    sumterm = sumterm + nchoosek(L-1+l, l)*((1+mu)/2).^l;
end
```

64

```matlab
qam64BerTheory = (4-4/sqrt(M))/log2(M)*((1-mu)/2).^L .* sumterm;
semilogy (EbN0_dB_QAM64, qam64BerTheory, 'g')

% QPSK
L=4;
iSNR = 10.^(Eb_N0_dB(1,:)/10)/L/2;
mu = sqrt(iSNR./(1+iSNR));
sumterm = 0;
for l=0:L-1
    sumterm = sumterm + nchoosek(L-1+l, l)*((1+mu)/2).^l;
end
qpskBerTheory = ((1-mu)/2).^L .* sumterm;
semilogy (EbN0_dB_QPSK, qpskBerTheory, 'g')

L=2;
iSNR = 10.^(Eb_N0_dB(1,:)/10)/L/2;
mu = sqrt(iSNR./(1+iSNR));
sumterm = 0;
for l=0:L-1
    sumterm = sumterm + nchoosek(L-1+l, l)*((1+mu)/2).^l;
end
qpskBerTheory = ((1-mu)/2).^L .* sumterm;
semilogy (EbN0_dB_QPSK, qpskBerTheory, 'g')


M=16;
L=2;
iSNR = 3*10.^(Eb_N0_dB(1,:)/10)/L/2/(M-1);
mu = sqrt(iSNR./(1+iSNR));
sumterm = 0;
for l=0:L-1
    sumterm = sumterm + nchoosek(L-1+l, l)*((1+mu)/2).^l;
end
qam16BerTheory = (4-4/sqrt(M))/log2(M)*((1-mu)/2).^L .* sumterm;
semilogy (EbN0_dB_QAM16, qam16BerTheory, 'g')

M=64;
L=2;
iSNR = 3*10.^(Eb_N0_dB(1,:)/10)/L/2/(M-1);
mu = sqrt(iSNR./(1+iSNR));
sumterm = 0;
for l=0:L-1
    sumterm = sumterm + nchoosek(L-1+l, l)*((1+mu)/2).^l;
end
qam64BerTheory = (4-4/sqrt(M))/log2(M)*((1-mu)/2).^L .* sumterm;
semilogy (EbN0_dB_QAM64, qam64BerTheory, 'g')
```

## ML_QO-STBC.m

This file is used to do the simulation of the QO-STBC with pairwise maximum likelihood decoding.

```matlab
clear
close all
load constellation_map

EsN0_lower = 0;
EsN0_upper = 40;
num_EsN0_points = 20;
num_points_per_iter = 4;

for modulation_type = 2:4

switch modulation_type
    case {1,2}
        m=modulation_type;
    case 3
        m=4;
    case 4
        m=6;
end

EsN0_dB = linspace(EsN0_lower,EsN0_upper,num_EsN0_points) ; % multiple Eb/N0 values
diversity_theory_curves
disp (sprintf('Simulating modulation type: %d', modulation_type));

% select modulation scheme
switch m
    case 1
        constellation_map = bpsk_map;
        c_factor = 1;
        N = logspace (log10(1e6),log10(2e8), num_EsN0_points); % number of bits or symbols

    case 2
        constellation_map = qpsk_map;
        c_factor = sqrt(2);
        angle = 0.599490699972004;
        N = max(1e4, floor(20/2./qpskBerTheory)); % number of bits or symbols
```

```matlab
            N(find(qpskBerTheory<1e-9)) = 0;
    case 4
            constellation_map = qam16_map;
            c_factor = sqrt(10);
            angle = 0.540396160267186;
            N = max(1e4, floor(20/4./qam16BerTheory)); % number of bits or symbols
            N(find(qam16BerTheory<1e-9)) = 0;
    case 6
            constellation_map = qam64_map;
            c_factor = sqrt(42);
            angle = 1.0360237298489;
            N = max(1e4, floor(20/6./qam64BerTheory)); % number of bits or symbols
            N(find(qam64BerTheory<1e-9)) = 0;
end

constellation_map2 = constellation_map .* exp(1i*angle);

% initialise variables
num_bit_errors_4xQO1 = zeros(1, num_EsN0_points);
num_sym_errors_4xQO1 = zeros(1, num_EsN0_points);
num_bit_errors_4xQO2 = zeros(1, num_EsN0_points);
num_sym_errors_4xQO2 = zeros(1, num_EsN0_points);
num_bit_errors_4xQO3 = zeros(1, num_EsN0_points);
num_sym_errors_4xQO3 = zeros(1, num_EsN0_points);
num_bit_errors_4xQO4 = zeros(1, num_EsN0_points);
num_sym_errors_4xQO4 = zeros(1, num_EsN0_points);


num_iter = ceil(N/num_points_per_iter/m);


tic
for j_iter = 1:num_EsN0_points
    currentBER = 1;
    for i_iter = 1:num_iter(j_iter)

        % Transmitter
        symbol_orig = randi([0 2^m-1],num_points_per_iter,1) ;
        s = constellation_map(symbol_orig+1);

        s_qo1 = s;
        s_qo1([3 4]) = s([3 4]) .* exp(1i*atan(0.5)/2);

        s_qo2 = s;

        s_qo3 = s;
        s_qo3([3 4]) = s([3 4]) .* exp(1i*pi()/4);

        s_qo4 = s;
        s_qo4([3 4]) = s([3 4]) .* exp(1i*angle);

        n = 1/sqrt(2)*(randn(num_points_per_iter*2,1) + 1i*randn(num_points_per_iter*2,1)); % white gaussian noise, 0dB
variance

        h1 = 1/sqrt(2)*(randn(1,1) + 1i*randn(1,1)); % Rayleigh channel
        h2 = 1/sqrt(2)*(randn(1,1) + 1i*randn(1,1)); % Rayleigh channel
        h3 = 1/sqrt(2)*(randn(1,1) + 1i*randn(1,1)); % Rayleigh channel
        h4 = 1/sqrt(2)*(randn(1,1) + 1i*randn(1,1)); % Rayleigh channel

        % instantaneous noise factior
        iNoiseFactor = 2*sqrt(2)*10^(-EsN0_dB(j_iter)/20);

        % Channel and noise Noise addition for QO
        H_4xQO = [              h1   h2    h3    h4
            -conj(h2)  conj(h1) -conj(h4)  conj(h3)
                      -h3     h4     h1   -h2
            -conj(h4) -conj(h3)  conj(h2)  conj(h1)];
        H_4xQO_13 = H_4xQO (:,[1 3]);
        H_4xQO_24 = H_4xQO (:,[2 4]);

        y_4xQO1 = H_4xQO * s_qo1 + iNoiseFactor*n(1:num_points_per_iter);
        y_4xQO2 = H_4xQO * s_qo2 + iNoiseFactor*n(1:num_points_per_iter);
        y_4xQO3 = H_4xQO * s_qo3 + iNoiseFactor*n(1:num_points_per_iter);
        y_4xQO4 = H_4xQO * s_qo4 + iNoiseFactor*n(1:num_points_per_iter);



        % receiver - do pairwise ML decoding for 4xQO, s1 and s3 are
        % orthogonal to s2 and s4, so decode them separately

        conmap_temp = constellation_map*ones(1,(2^m));
        conmap2_temp = constellation_map*exp(1i*atan(0.5)/2)*ones(1,(2^m));
        pairwise_vector = [reshape(conmap_temp, 1, 2^(2*m)); reshape(conmap2_temp.', 1, 2^(2*m))];
        [dummy,ind]=min(sum(abs(y_4xQO1*ones(1,2^(2*m)) - H_4xQO_24*pairwise_vector).^2));
        symbol_4xQO1(4) = floor((ind-1)/2^m);
        symbol_4xQO1(2) = mod (ind-1, 2^m);
        [dummy,ind]=min(sum(abs(y_4xQO1*ones(1,2^(2*m)) - H_4xQO_13*pairwise_vector).^2));
        symbol_4xQO1(3) = floor((ind-1)/2^m);
        symbol_4xQO1(1) = mod (ind-1, 2^m);

        conmap_temp = constellation_map*ones(1,(2^m));
        conmap2_temp = conmap_temp;
        pairwise_vector = [reshape(conmap_temp, 1, 2^(2*m)); reshape(conmap2_temp.', 1, 2^(2*m))];
```

66

```matlab
            [dummy,ind]=min(sum(abs(y_4xQO2*ones(1,2^(2*m)) - H_4xQO_24*pairwise_vector).^2));
            symbol_4xQO2(4) = floor((ind-1)/2^m);
            symbol_4xQO2(2) = mod (ind-1, 2^m);
            [dummy,ind]=min(sum(abs(y_4xQO2*ones(1,2^(2*m)) - H_4xQO_13*pairwise_vector).^2));
            symbol_4xQO2(3) = floor((ind-1)/2^m);
            symbol_4xQO2(1) = mod (ind-1, 2^m);

            conmap_temp = constellation_map*ones(1,(2^m));
            conmap2_temp = constellation_map*exp(1i*pi()/4)*ones(1,(2^m));
            pairwise_vector = [reshape(conmap_temp, 1, 2^(2*m)); reshape(conmap2_temp.', 1, 2^(2*m))];
            [dummy,ind]=min(sum(abs(y_4xQO3*ones(1,2^(2*m)) - H_4xQO_24*pairwise_vector).^2));
            symbol_4xQO3(4) = floor((ind-1)/2^m);
            symbol_4xQO3(2) = mod (ind-1, 2^m);
            [dummy,ind]=min(sum(abs(y_4xQO3*ones(1,2^(2*m)) - H_4xQO_13*pairwise_vector).^2));
            symbol_4xQO3(3) = floor((ind-1)/2^m);
            symbol_4xQO3(1) = mod (ind-1, 2^m);

            conmap_temp = constellation_map*ones(1,(2^m));
            conmap2_temp = constellation_map2*ones(1,(2^m));
            pairwise_vector = [reshape(conmap_temp, 1, 2^(2*m)); reshape(conmap2_temp.', 1, 2^(2*m))];
            [dummy,ind]=min(sum(abs(y_4xQO4*ones(1,2^(2*m)) - H_4xQO_24*pairwise_vector).^2));
            symbol_4xQO4(4) = floor((ind-1)/2^m);
            symbol_4xQO4(2) = mod (ind-1, 2^m);
            [dummy,ind]=min(sum(abs(y_4xQO4*ones(1,2^(2*m)) - H_4xQO_13*pairwise_vector).^2));
            symbol_4xQO4(3) = floor((ind-1)/2^m);
            symbol_4xQO4(1) = mod (ind-1, 2^m);


            % count bit errors
            dummy = (constellation_map(symbol_orig+1)-constellation_map(symbol_4xQO1+1)) * c_factor/2;
            num_bit_errors_4xQO1(j_iter) = num_bit_errors_4xQO1(j_iter) + sum(bit_diff_map(round(abs(real(dummy)))+1)) +
sum(bit_diff_map(round(abs(imag(dummy)))+1));
            dummy = (constellation_map(symbol_orig+1)-constellation_map(symbol_4xQO2+1)) * c_factor/2;
            num_bit_errors_4xQO2(j_iter) = num_bit_errors_4xQO2(j_iter) + sum(bit_diff_map(round(abs(real(dummy)))+1)) +
sum(bit_diff_map(round(abs(imag(dummy)))+1));
            dummy = (constellation_map(symbol_orig+1)-constellation_map(symbol_4xQO3+1)) * c_factor/2;
            num_bit_errors_4xQO3(j_iter) = num_bit_errors_4xQO3(j_iter) + sum(bit_diff_map(round(abs(real(dummy)))+1)) +
sum(bit_diff_map(round(abs(imag(dummy)))+1));
            dummy = (constellation_map(symbol_orig+1)-constellation_map(symbol_4xQO4+1)) * c_factor/2;
            num_bit_errors_4xQO4(j_iter) = num_bit_errors_4xQO4(j_iter) + sum(bit_diff_map(round(abs(real(dummy)))+1)) +
sum(bit_diff_map(round(abs(imag(dummy)))+1));


            if mod (i_iter, 500)==1
                if j_iter>1
                    secs_left = toc/(i_iter+sum(num_iter(1:j_iter-1)))  *   (num_iter(j_iter)-i_iter +
sum(num_iter(j_iter+1:num_EsN0_points)));
                else
                    secs_left = toc/(i_iter)*(sum(num_iter(j_iter+1:num_EsN0_points)));
                end
                disp(sprintf('Estimated time remaining: %f seconds, ETA: %s', secs_left, datestr(now+secs_left/86400)))
                disp(sprintf('Mod: %d,  Current EbN0: %.1f (%d%%), current BER: %e', modulation_type, EsN0_dB(j_iter),
floor(i_iter/num_iter(j_iter)*100), num_bit_errors_4xQO4(j_iter)/m/num_points_per_iter/i_iter   ))

            end
        end
end
N = num_iter * num_points_per_iter;

simBer_4xQO1(modulation_type,:) = num_bit_errors_4xQO1./N/m; % simulated ber
simBer_4xQO2(modulation_type,:) = num_bit_errors_4xQO2./N/m; % simulated ber
simBer_4xQO3(modulation_type,:) = num_bit_errors_4xQO3./N/m; % simulated ber
simBer_4xQO4(modulation_type,:) = num_bit_errors_4xQO4./N/m; % simulated ber

end

EbN0_dB_QPSK = EsN0_dB - 10*log10(2);
EbN0_dB_QAM16 = EsN0_dB - 10*log10(4);
EbN0_dB_QAM64 = EsN0_dB - 10*log10(6);

EbN0_dB = [EsN0_dB; EbN0_dB_QPSK; EbN0_dB_QAM16; EbN0_dB_QAM64];

filename = ['myrun_QO_final_' num2str(now) '.mat'];
save (filename)

% plot
close all
figure
for i=2:4
    semilogy(EbN0_dB(i,:),simBer_4xQO1(i,:),'rx-','LineWidth',2);
    hold on
end
for i=2:4
    semilogy(EbN0_dB(i,:),simBer_4xQO2(i,:),'bx-','LineWidth',2);
    hold on
end
for i=2:4
    semilogy(EbN0_dB(i,:),simBer_4xQO3(i,:),'kx-','LineWidth',2);
    hold on
end
for i=2:4
    semilogy(EbN0_dB(i,:),simBer_4xQO4(i,:),'gx-','LineWidth',2);
    hold on
```

```
    end

axis([EsN0_lower 40 10^-6 0.5])
grid on
xlabel('Eb/No, dB');
ylabel('Bit Error Rate');


% calculate theoretical QAM curves
M=16;
L=4;
iSNR = 3*10.^(EbN0_dB(1,:)/10)/L/2/(M-1);
mu = sqrt(iSNR./(1+iSNR));
sumterm = 0;
for l=0:L-1
    sumterm = sumterm + nchoosek(L-1+l, l)*((1+mu)/2).^l;
end
qam16BerTheory = (4-4/sqrt(M))/log2(M)*((1-mu)/2).^L .* sumterm;
semilogy (EbN0_dB_QAM16, qam16BerTheory, 'y','LineWidth',1)

M=64;
L=4;
iSNR = 3*10.^(EbN0_dB(1,:)/10)/L/2/(M-1);
mu = sqrt(iSNR./(1+iSNR));
sumterm = 0;
for l=0:L-1
    sumterm = sumterm + nchoosek(L-1+l, l)*((1+mu)/2).^l;
end
qam64BerTheory = (4-4/sqrt(M))/log2(M)*((1-mu)/2).^L .* sumterm;
semilogy (EbN0_dB_QAM64, qam64BerTheory, 'y','LineWidth',1)

% QPSK
L=4;
iSNR = 10.^(EbN0_dB(1,:)/10)/L/2;
mu = sqrt(iSNR./(1+iSNR));
sumterm = 0;
for l=0:L-1
    sumterm = sumterm + nchoosek(L-1+l, l)*((1+mu)/2).^l;
end
qpskBerTheory = ((1-mu)/2).^L .* sumterm;
semilogy (EbN0_dB_QPSK, qpskBerTheory, 'y','LineWidth',1)
```

## `cdm_plot.m`

This file is used to calculate the determinant of the code difference matrix for various modulation schemes.

```
clear
close all
load constellation_map

m=2;


switch m
    case 1
        constellation_map = bpsk_map;
        c_factor = 1;
    case 2
        constellation_map = qpsk_map;
        c_factor = sqrt(2);
    case 4
        constellation_map = qam16_map;
        c_factor = sqrt(10);
    case 6
        constellation_map = qam64_map;
        c_factor = sqrt(42);
end

num_points = 2000;
angles = linspace(0,90,num_points);
num_points = length(angles);


zero_eigs_count = 0;
min_div_prod = zeros(num_points,1);

tic
for current_angle=1:num_points

    constellation_map2 = constellation_map * exp(1i * (angles(current_angle) / 180 * pi));
    current_min = realmax;

    for i=0:((2^m)^2)-2
        current_set2_length = ((2^m)^2)-1-i;

        set1 = zeros(2,1);
        set2 = zeros(2, current_set2_length);
```

```
            j = i+1:((2^m)^2)-1;

            setcombination1 = i;
            setcombination2 = j';

            for k=1:2
                set1(k) = mod(setcombination1, 2^m);
                set2(k, :) = mod(setcombination2, 2^m);
                setcombination1 = floor (setcombination1/2^m);
                setcombination2 = floor (setcombination2/2^m);
            end
            set1 = kron(set1, ones(1, current_set2_length));

            s1 = constellation_map(set1+1);
            s2 = constellation_map(set2+1);

            s1(2, :) = constellation_map2(set1(2,:)+1);
            s2(2, :) = constellation_map2(set2(2,:)+1);


            a = sum( (s1-s2).^2   );
            current_min = min([current_min, 1/4 * sqrt(abs(a)) ]   );

        end
        min_div_prod(current_angle) = current_min;

        plot (angles, min_div_prod)
        title (['Min diversity: ' num2str(min_div_prod(current_angle)) ], 'FontSize', 14);
        xlabel ('Angle in degrees')
        ylabel ('Diversity')

        drawnow
        secsleft = toc/current_angle * (num_points-current_angle);
        disp (sprintf('Estimated time left: %f, ETA: %s', secsleft, datestr(now+secsleft/86400)));

end
```

## freq_div.m

This file is used to simulate the frequency diversity scheme using space-time-frequency code

```
clear
close all
load constellation_map

EsN0_lower = 3;
EsN0_upper = 45;
num_EsN0_points = 25;
num_points_per_iter = 6e4;

simBer_2x1 = zeros(4, num_EsN0_points);
simBer_2x2_flat = zeros(4, num_EsN0_points);
simBer_2x2_selective = zeros(4, num_EsN0_points);
simBer_2x2_50corr = zeros(4, num_EsN0_points);
simBer_2x2_90corr = zeros(4, num_EsN0_points);


for modulation_type = 2:4

    N = logspace (log10(1e7),log10(1e10), num_EsN0_points); % number of bits or symbols


% modulation_type=2;
switch modulation_type
    case {1,2}
        m=modulation_type;
    case 3
        m=4;
    case 4
        m=6;
end

num_iter = ceil(N/num_points_per_iter/m);



% m=2;
% select modulation scheme

disp (sprintf('Simulating modulation type: %d', modulation_type));
switch m
    case 1
        constellation_map = bpsk_map;
```

```matlab
            c_factor = 1;
        case 2
            constellation_map = qpsk_map;
            c_factor = sqrt(2);
        case 4
            constellation_map = qam16_map;
            c_factor = sqrt(10);
        case 6
            constellation_map = qam64_map;
            c_factor = sqrt(42);
end


% initialise variables
EsN0_dB = linspace(EsN0_lower,EsN0_upper,num_EsN0_points) ; % multiple Eb/N0 values

num_bit_errors_2x1 = zeros(1, num_EsN0_points);
num_bit_errors_2x2_flat = zeros(1, num_EsN0_points);
num_bit_errors_2x2_selective = zeros(1, num_EsN0_points);
num_bit_errors_2x2_50corr = zeros(1, num_EsN0_points);
num_bit_errors_2x2_90corr = zeros(1, num_EsN0_points);

EbN0_dB_QPSK = EsN0_dB - 10*log10(2);
EbN0_dB_QAM16 = EsN0_dB - 10*log10(4);
EbN0_dB_QAM64 = EsN0_dB - 10*log10(6);

EbN0_dB = [EsN0_dB; EbN0_dB_QPSK; EbN0_dB_QAM16; EbN0_dB_QAM64];


tic
for j_iter = 1:num_EsN0_points
    for i_iter = 1:num_iter(j_iter)
        % Transmitter
        symbol_orig = randi([0 2^m-1],num_points_per_iter,1) ;
        s = constellation_map(symbol_orig+1);


        n1 = 1/sqrt(2)*(randn(num_points_per_iter,1) + 1i*randn(num_points_per_iter,1)); % white gaussian noise, 0dB
variance
        n2 = 1/sqrt(2)*(randn(num_points_per_iter,1) + 1i*randn(num_points_per_iter,1)); % white gaussian noise, 0dB
variance
        n3 = 1/sqrt(2)*(randn(num_points_per_iter,1) + 1i*randn(num_points_per_iter,1)); % white gaussian noise, 0dB
variance
        n4 = 1/sqrt(2)*(randn(num_points_per_iter,1) + 1i*randn(num_points_per_iter,1)); % white gaussian noise, 0dB
variance


        h1 = 1/sqrt(2)*(randn(num_points_per_iter,1) + 1i*randn(num_points_per_iter,1)); % Rayleigh channel
        h2 = 1/sqrt(2)*(randn(num_points_per_iter,1) + 1i*randn(num_points_per_iter,1)); % Rayleigh channel
        h3 = 1/sqrt(2)*(randn(num_points_per_iter,1) + 1i*randn(num_points_per_iter,1)); % Rayleigh channel
        h4 = 1/sqrt(2)*(randn(num_points_per_iter,1) + 1i*randn(num_points_per_iter,1)); % Rayleigh channel


        h3_50corr = h1 * 0.5 + sqrt (1-0.5^2) * h3;
        h4_50corr = h2 * 0.5 + sqrt (1-0.5^2) * h4;

        h3_90corr = h1 * 0.9 + sqrt (1-0.9^2) * h3;
        h4_90corr = h2 * 0.9 + sqrt (1-0.9^2) * h4;

        % Channel and noise Noise addition
        noiseFactor = sqrt(2)*(10^(-EsN0_dB(j_iter)/20));

        y_2x1 = s             + noiseFactor.*        (conj(h1).*n1   +  h2.*n2 ) ./ (h1.*conj(h1) + h2.*conj(h2));
        y_2x2_flat = s        + noiseFactor.*        (conj(h1).*n1   +  h2.*n2 + conj(h1).*n3   +  h2.*n4) ./
(2*h1.*conj(h1) + 2*h2.*conj(h2));
        y_2x2_selective = s   + noiseFactor.*        (conj(h1).*n1   +  h2.*n2 + conj(h3).*n3   +  h4.*n4) ./
(h1.*conj(h1) + h2.*conj(h2) + h3.*conj(h3) + h4.*conj(h4));
        y_2x2_50corr = s      + noiseFactor.*        (conj(h1).*n1   +  h2.*n2 + conj(h3_50corr).*n3   +
h4_50corr.*n4) ./ (h1.*conj(h1) + h2.*conj(h2) + h3_50corr.*conj(h3_50corr) + h4_50corr.*conj(h4_50corr));
        y_2x2_90corr = s      + noiseFactor.*        (conj(h1).*n1   +  h2.*n2 + conj(h3_90corr).*n3   +
h4_90corr.*n4) ./ (h1.*conj(h1) + h2.*conj(h2) + h3_90corr.*conj(h3_90corr) + h4_90corr.*conj(h4_90corr));


        % receiver - hard decision symbol decoding
        [dummy, sort_index] = sort (abs(constellation_map*ones(1,num_points_per_iter) - ones(2^m,1)*y_2x1.'));
        symbol_2x1 = sort_index(1,:).'-1;
        [dummy, sort_index] = sort (abs(constellation_map*ones(1,num_points_per_iter) - ones(2^m,1)*y_2x2_flat.'));
        symbol_2x2_flat = sort_index(1,:).'-1;
        [dummy, sort_index] = sort (abs(constellation_map*ones(1,num_points_per_iter) -
ones(2^m,1)*y_2x2_selective.'));
        symbol_2x2_selective = sort_index(1,:).'-1;
        [dummy, sort_index] = sort (abs(constellation_map*ones(1,num_points_per_iter) - ones(2^m,1)*y_2x2_50corr.'));
        symbol_2x2_50corr = sort_index(1,:).'-1;
        [dummy, sort_index] = sort (abs(constellation_map*ones(1,num_points_per_iter) - ones(2^m,1)*y_2x2_90corr.'));
        symbol_2x2_90corr = sort_index(1,:).'-1;

        % count bit errors
        dummy = (s-constellation_map(symbol_2x1+1)) * c_factor/2;
        num_bit_errors_2x1(j_iter) = num_bit_errors_2x1(j_iter) + sum(bit_diff_map(round(abs(real(dummy)))+1)) +
sum(bit_diff_map(round(abs(imag(dummy)))+1));
        dummy = (s-constellation_map(symbol_2x2_flat+1)) * c_factor/2;
```

```matlab
            num_bit_errors_2x2_flat(j_iter) = num_bit_errors_2x2_flat(j_iter) +
sum(bit_diff_map(round(abs(real(dummy)))+1)) + sum(bit_diff_map(round(abs(imag(dummy)))+1));
            dummy = (s-constellation_map(symbol_2x2_selective+1)) * c_factor/2;
            num_bit_errors_2x2_selective(j_iter) = num_bit_errors_2x2_selective(j_iter) +
sum(bit_diff_map(round(abs(real(dummy)))+1)) + sum(bit_diff_map(round(abs(imag(dummy)))+1));
            dummy = (s-constellation_map(symbol_2x2_50corr+1)) * c_factor/2;
            num_bit_errors_2x2_50corr(j_iter) = num_bit_errors_2x2_50corr(j_iter) +
sum(bit_diff_map(round(abs(real(dummy)))+1)) + sum(bit_diff_map(round(abs(imag(dummy)))+1));
            dummy = (s-constellation_map(symbol_2x2_90corr+1)) * c_factor/2;
            num_bit_errors_2x2_90corr(j_iter) = num_bit_errors_2x2_90corr(j_iter) +
sum(bit_diff_map(round(abs(real(dummy)))+1)) + sum(bit_diff_map(round(abs(imag(dummy)))+1));


        if mod (i_iter, 10)==1

            currentBER_2x2f = num_bit_errors_2x2_flat(j_iter)/m/num_points_per_iter/i_iter;
            currentBER_2x2s = num_bit_errors_2x2_selective(j_iter)/m/num_points_per_iter/i_iter;
            currentBER_2x1 = num_bit_errors_2x1(j_iter)/m/num_points_per_iter/i_iter;

            biterr_limit2x2s = max(1, (currentBER_2x2s*1e9)^0.65);
            biterr_limit2x2f = max(1, (currentBER_2x2f*1e9)^0.65);


            if j_iter>1
                secs_left = toc/(i_iter+sum(num_iter(1:j_iter-1)))  *   (num_iter(j_iter)-i_iter +
sum(num_iter(j_iter+1:num_EsN0_points))) ;
            else
                secs_left = toc/(i_iter)*(num_iter(j_iter)-i_iter + sum(num_iter(j_iter+1:num_EsN0_points)));
            end
            disp(sprintf('Estimated time remaining: %.1f seconds (%d, %.1f%%), ETA: %s', secs_left, j_iter,
i_iter/num_iter(j_iter)*100, datestr(now+secs_left/86400)))
            disp(sprintf('2x2s BER: %e, Bit errors: %d, Limits: %.1f', currentBER_2x2s,
num_bit_errors_2x2_selective(j_iter), biterr_limit2x2s))
            disp(sprintf('2x2f BER: %e, Bit errors: %d, Limits: %.1f', currentBER_2x2f,
num_bit_errors_2x2_flat(j_iter), biterr_limit2x2f))
            disp(sprintf('2x1  BER: %e, Bit errors: %d', currentBER_2x1, num_bit_errors_2x1(j_iter)))



            if (currentBER_2x2s > 5e-7 && num_bit_errors_2x2_selective(j_iter) >= biterr_limit2x2s ) || ...
                    (num_bit_errors_2x1(j_iter) > 5 && currentBER_2x1 < 5e-7 ) || ...
                    (currentBER_2x2s < 5e-7 && num_bit_errors_2x2_flat(j_iter) >= biterr_limit2x2f   )
                num_iter(j_iter) = i_iter;
                if (num_bit_errors_2x1(j_iter) > 5 && currentBER_2x1 < 5e-7 )
                    num_iter(j_iter+1:num_EsN0_points)=0;
                end
                break
            end

        end
    end

    if currentBER_2x1 > 5e-7
        simBer_2x1(modulation_type,j_iter) = num_bit_errors_2x1(j_iter)./num_points_per_iter/i_iter/m; % simulated ber
        simBer_2x2_flat(modulation_type,j_iter) = num_bit_errors_2x2_flat(j_iter)./num_points_per_iter/i_iter/m; %
simulated ber
        simBer_2x2_selective(modulation_type,j_iter) =
num_bit_errors_2x2_selective(j_iter)./num_points_per_iter/i_iter/m; % simulated ber
        simBer_2x2_50corr(modulation_type,j_iter) = num_bit_errors_2x2_50corr(j_iter)./num_points_per_iter/i_iter/m; %
simulated ber
        simBer_2x2_90corr(modulation_type,j_iter) = num_bit_errors_2x2_90corr(j_iter)./num_points_per_iter/i_iter/m; %
simulated ber

        semilogy(EbN0_dB(modulation_type,:),simBer_2x1(modulation_type,:),'rx-','LineWidth',1);
        hold on

        semilogy(EbN0_dB(modulation_type,:),simBer_2x2_flat(modulation_type,:),'bx-','LineWidth',1);
        hold on

        semilogy(EbN0_dB(modulation_type,:),simBer_2x2_selective(modulation_type,:),'mx-','LineWidth',1);
        hold on

        semilogy(EbN0_dB(modulation_type,:),simBer_2x2_90corr(modulation_type,:),'gx-','LineWidth',1);
        hold on

        semilogy(EbN0_dB(modulation_type,:),simBer_2x2_50corr(modulation_type,:),'kx-','LineWidth',1);
        hold on

        axis([0 40 10^-6 0.5])
        grid on
        legend('2x1', '2x2-flat', '2x2-selective', '2x2-90corr', '2x2-50corr');
        xlabel('Eb/No, dB');
        ylabel('Bit Error Rate');
        title('BER for BPSK modulation in Rayleigh channel');

        drawnow
    end
end
N = num_iter * num_points_per_iter;

simBer_2x1(modulation_type,:) = num_bit_errors_2x1./N/m; % simulated ber
simBer_2x2_flat(modulation_type,:) = num_bit_errors_2x2_flat./N/m; % simulated ber\
simBer_2x2_selective(modulation_type,:) = num_bit_errors_2x2_selective./N/m; % simulated ber\
```

```
simBer_2x2_50corr(modulation_type,:) = num_bit_errors_2x2_50corr./N/m; % simulated ber\
simBer_2x2_90corr(modulation_type,:) = num_bit_errors_2x2_90corr./N/m; % simulated ber\


end


filename = ['fec_test3_with50corr' num2str(now) '.mat'];
save (filename)

% plot
close all
figure

for i=2:4
    semilogy(EbN0_dB(i,:),simBer_2x1(i,:),'rx-','LineWidth',1);
    hold on
end
for i=2:4
    semilogy(EbN0_dB(i,:),simBer_2x2_flat(i,:),'bx-','LineWidth',1);
    hold on
end
for i=2:4
    semilogy(EbN0_dB(i,:),simBer_2x2_selective(i,:),'mx-','LineWidth',1);
    hold on
end
for i=2:4
    semilogy(EbN0_dB(i,:),simBer_2x2_90corr(i,:),'gx-','LineWidth',1);
    hold on
end
for i=2:4
    semilogy(EbN0_dB(i,:),simBer_2x2_50corr(i,:),'kx-','LineWidth',1);
    hold on
end

axis([0 40 10^-6 0.5])
grid on
legend('2x1', '2x2-flat', '2x2-selective', '2x2-90corr', '2x2-50corr');
xlabel('Eb/No, dB');
ylabel('Bit Error Rate');
title('BER for QPSK modulation');
```

## freq_corr_analysis.m

This file is used to analyse the correlation between frequency responses for the COST 207 six-ray TU model

```
close all
clear

% COST 207 TU model
delays = [0 0.2 0.5 1.6 2.3 5.0]*1e-6
power = [0.189 0.379 0.239 0.095 0.061 0.037]
power_db = 10*log10(power)

% plot the impulse response
figure
set(gcf,'PaperPositionMode','auto')
stem(delays,power)
title('Impulse response of the COST 207 TU model')
xlabel('Time in seconds')
ylabel('Fractional Power')


% calculate coherence bandwidth
mean_delay = sum(delays .* power) / sum(power)
tau2 = sum(delays.^2 .* power) / sum(power)
delay_spread = sqrt(tau2 - mean_delay.^2)
Bc = 1/(5*delay_spread)

% num_freq_points = 1000;
f = 0:1e4:1e6;

num_random_points = 1e6;
num_freq_points = length(f);
chan_gain = zeros(num_random_points, num_freq_points);

tic
for i=1:num_random_points
    chan = rayleighchan (1e-6, 0, delays, power_db);

    Hf = sum(kron(chan.PathGains.', ones(1,num_freq_points)) .* exp(-1i * 2*pi * delays.' * f));
%    plot (f, abs(Hf))

    chan_gain(i,:) = abs(Hf);
```

```matlab
    if mod(i, 10) == 1
        secs_left = toc/i   *   (num_random_points-i);
        disp(sprintf('Estimated time remaining: %.1f secs, ETA: %s', secs_left, datestr(now+secs_left/86400)))
    end

end

corr_vec = zeros(1,num_freq_points);
for i=1:num_freq_points
    corr_vec(i) = corr(chan_gain(:,1), chan_gain(:,i));
end

% plot the correlation figure
figure
set(gcf,'PaperPositionMode','auto')
plot (f, corr_vec, 'LineWidth', 1)
axis([f(1) f(end) 0 1])
title('Correlation between frequencies for the COST 207 TU model')
xlabel('Frequency separation, \Deltaf in Hz')
ylabel('Correlation coefficient')
grid on
```

THIS PAGE INTENTIONALLY LEFT BLANK

# LIST OF REFERENCES

[1]     T. T. Ha, *Theory and Design of Digital Communication Systems*, Cambridge University Press, 2011.

[2]     A. Goldsmith, *Wireless Communications*, Cambridge University Press, p. 89, Aug. 2005.

[3]     J. Proakis, *Digital Communications*, McGraw-Hill Science, 4th Edition, 2000.

[4]     S.M. Alamouti, "A Simple Transmit Diversity Technique for Wireless Communications," *IEEE Journal on Selected Areas In Communications*, vol. 16, no. 8, pp. 1451–1458, Oct. 1998.

[5]     V. Tarokh, H. Jafarkhani, and A. R. Calderbank, "Space–Time Block Codes From Orthogonal Designs," *IEEE Transactions on Information Theory*, vol. 45, no. 5, pp. 1456–1467, Jul. 1999.

[6]     B. Badic, M. Rupp and H. Weinrichter, "Quasi-Orthogonal Space-Time Block Codes: Approaching Optimality," *Proceedings in EUSIPCO European Signal Processing Conference*, Anatalya, Turkey, Sep. 2005.

[7]     H. Jafarkhani, "A Quasi-Orthogonal Space-Time Block Code," *IEEE Transactions on Communications*, vol. 49, no. 1, pp. 1–4, Jan. 2001.

[8]     N. Sharma and C.B. Papadias, "Improved Quasi-Orthogonal Codes Through Constellation Rotation," *IEEE International Conference on Acoustics, Speech, and Signal Processing*, vol. 4, pp. IV-3968 – IV-3971, 2002.

[9]     W. Su and X. Xia, "Signal Constellations for Quasi-Orthogonal Space-Time Block Codes With Full Diversity," *IEEE Transactions on Information Theory*, vol. 50, no. 10, pp. 2331–2347, Oct. 2004.

[10]    H. Wang, D. Wang and X. Xia, "On Optimal Quasi-Orthogonal Space-Time Block Codes With Minimum Decoding Complexity," *IEEE Transactions on Information Theory*, vol. 55, no. 3, pp. 1104–1130, Mar. 2009.

[11]    C. Yuan, Y. L. Guan and T. T. Tjhung, "Quasi-Orthogonal STBC With Minimum Decoding Complexity," *IEEE Transactions on Wireless Communications*, vol. 4, no. 5, pp. 2089–2094, Sep. 2005.

[12]    V. Tarokh, N. Seshadri and A. R. Calderbank, "Space-Time Codes for High Data Rate Wireless Communication: Performance Criterion and Code Construction," *IEEE Transactions on Information Theory*, vol. 44, no. 2, pp. 744–765, Mar. 1998.

[13]   W. Su, Z. Safar, M. Olfat and K. J. R. Liu, "Obtaining Full-Diversity Space-Frequency Codes From Space-Time Codes via Mapping," *IEEE Transactions on Signal Processing*, vol. 51, no. 11, pp. 2905–2916, Nov. 2003.

[14]   Z. Liu, Y. Xin and G. B. Giannakis, "Space-Time-Frequency Coded OFDM Over Frequency-Selective Fading Channels," *IEEE Transactions on Signal Processing*, vol. 50, no. 10, pp. 2465–2476, Oct. 2002.

[15]   H. Bolcskei and A. J. Paulraj, "Space-Frequency Coded Broadband OFDM Systems," *Wireless Communications and Networking Conference, 2000. WCNC. 2000 IEEE,* vol. 1, pp. 1–6, 2000.

[16]   A. F. Molisch, M. Z. Win and J. H. Winters, "Space-time-frequency (STF) coding for MIMO-OFDM systems," *IEEE Communications Letters*, vol.6, no.9, pp. 370–372, Sep. 2002.

[17]   W. Su, Z. Safar and K. J. R. Liu, "Towards Maximum Achievable Diversity in Space, Time and Frequency: Performance Analysis and Code Design," *IEEE Transactions on Wireless Communications*, vol. 4, no. 4, pp. 1847–1857, Jul. 2005.

[18]   W. Zhang, X. Xia and P.C. Ching, "High-Rate Full-Diversity Space-Time-Frequency Codes for Broadband MIMO Block-Fading Channels," *IEEE Transactions on Communications*, vol. 55, no. 1, pp. 25–34, Jan. 2007.

[19]   E. Haas, "Multipath propagation," Image, last accessed Oct. 9, 2010, http://www.kn-s.dlr.de/People/Haas/

[20]   COST 207, *Digital land mobile radio communications*, Office for Official Publications of the European Communities, Final report, Luxembourg, 1989.

[21]   W. Jakes, *Microwave Mobile Communications*, Wiley-Interscience, 1974.

[22]   B. Vucetic and J. Yuan, *Space-Time Coding*, Wiley, 2003.

[23]   "IEEE Standard for Local and metropolitan area networks Part 16: Air Interface for Broadband Wireless Access Systems," *IEEE Std 802.16-2009 (Revision of IEEE Std 802.16-2004)*, pp. C1-2004, May. 29 2009.

# INITIAL DISTRIBUTION LIST

1.  Defense Technical Information Center
    Ft. Belvoir, Virginia

2.  Dudley Knox Library
    Naval Postgraduate School
    Monterey, California

3.  Chairman, Code EC
    Department of Electrical and Computer Engineering
    Naval Postgraduate School
    Monterey, California

4.  Tri T. Ha
    Naval Postgraduate School
    Monterey, California

5.  Weilian Su
    Naval Postgraduate School
    Monterey, California

6.  Tat Soon Yeo
    Temasek Defence Systems Institute (TDSI)
    National University of Singapore
    Singapore

7.  Tan Lai Poh
    Temasek Defence Systems Institute (TDSI)
    National University of Singapore
    Singapore

8.  Ng Wei Gee
    Naval Postgraduate School
    Monterey, California